SUPPORTING INFORMATION

Phenylphosphonic acid corroles: corroles that link and bind

Gaëlle Divoux, Margerie Loze, Yoann Rousselin, Stéphane Brandès, Claude P. Gros, Nicolas Desbois and Laurie André

Table of Contents

Materials and Methods

All starting reagents and solvents were purchased from commercial suppliers and were used without further purification, unless otherwise stated: Dichloromethane (DCM), dimethyl sulfoxide (DMSO), were purchased from Carlo ERBA®. Methanol (MeOH), hydrochloric acid (HCl) (37%), tetrahydrofuran (THF), acetone, ammonia 25% (NH_3) were purchased from VWR chemicals®. Chloroform ($CHCl_3$), dimethylformamide (DMF), ethyl acetate (AcOEt), anhydrous sodium sulfate and toluene were purchased from Fisher Scientifics®. DMF was dried over 3 Å molecular sieves. Cobalt acetylacetonate ($Co(acac)_2$) and diethylphosphite were purchased from Sigma-Aldrich®. *p*-Chloranil was purchased from Alfa Aesar®. Zirconium dichloride oxide and dichloroacetic acid (DAA) were purchased from Acros Organics®. The THF without stabilizer was obtain from the solvent purification system (PureSolv) of Innovative Technology. 4-Bromobenzaldehyde, bromotrimethylsilane were purchased from Tokyo Chemical Industry. Column chromatography purification was carried out on silica gel (Silica 60, 40-63 μm VWR chemicals®). Analytical thin-layer chromatography (TLC) was carried out using Merck silica gel 60 F-254 plates (precoated sheets, 0.2 mm thick, with fluorescence indicator F254). Porphyrins and corroles reported herein were synthesized at the ICMUB laboratory in Dijon (France). Their synthesis and characterizations are presented in this Electronic Supplementary Information (ESI). All spectrometers and diffractometers were available at the "Pôle de Chimie Moléculaire", the technological platform for chemical analysis and molecular synthesis (http://www.wpcm.fr) which relies on the Institute of the Molecular Chemistry of Univ. Bourgogne Europe (UBE) and Sayens™, an UBE private subsidiary.

^{1}H, ^{31}P and ^{19}F NMR. NMR spectra were acquired on a Bruker Avance III Nanobay 400 MHz and 500 MHz and chemical shifts (δ) of proton and fluor were expressed in ppm relative to deuterated dimethyl sulfoxide (DMSO-d_6, δ_H 2.50), deuterated methanol (CD_3OD, δ_H 3.31) or to chloroform ($CHCl_3$, δ_H 7.26).

MOFs ^{1}H NMR. MOF, previously dried, were digested and return to starting carboxylic acid derivatives (porphyrins and corroles) by adding on the material suspended in DMSO, two drops of deuterium chloride (D_2O.DCl) and 1 mg of sodium fluoride (NaF). Then, ^{1}H NMR spectra were acquired after complete MOF decomposition.

UV-Visible spectroscopy. UV-Visible spectra were acquired on an Agilent Cary 60 spectrophotometer in the 300-800 nm range and a scan rate of 600 nm/min. All measurements were carried out at room temperature in MeOH or DCM at three different concentrations done at following: 5 mg of the products were dissolved in 25 mL MeOH or DCM to obtained a first mother solution S_0. Then S_1 S_2 and S_3 solutions were obtained by diluting 3 mL, 4 mL and 5 mL of S_0 in 100 mL thanks to adapted volumetric flasks.

Infrared spectroscopy. FTIR spectra were recorded on a FTIR BRUKER Vertex 70v spectrometer in ATR mode.

Mass spectrometry. Low resolution Mass Spectra were recorded on a BRUKER MicroFlex® spectrometer in the MALDI-TOF reflection mode and by using dithranol as matrix.

High resolution mass spectroscopy (HR-MS). HR-MS spectra were recorded on a Thermo Scientific LTQ Orbitrap XL instrument in the ESI mode.

Powder X-Ray diffraction (PXRD). PXRD experiments were performed on an PANalytical Empyrean diffractometer in the range of $2\ ° < 2\theta < 50\ °$. Uncrushed samples were placed between two Mylar sheets and analyses were performed in transmission mode using a focusing X-ray mirror equipped with fixed divergent and anti-scattering slits (aperture 0.5 °) and 0.02 rad Soller slits. Data collection was run with a copper anticathode X-ray tube ($CuK\alpha_1$ = 1.54060 Å / $CuK\alpha_2$ = 1.54443 Å) and with a PIXcel1D detector equipped with an anti-scattering slit of 5 mm. Le Bail refinement was executed using the software Jana2006 ver. 23.05.2022.

Metal ions analyses. Metal ions analyses were performed on an ICP-AES iCAP 7400 of the digested materials in concentrated HNO_3.

Nitrogen adsorption/desorption. Nitrogen adsorption and desorption isotherms were measured at 77 K on a Micromeritics ASAP 2020 instrument or on a Belsorp maxII apparatus. The residual solvent molecules trapped inside the pores of the solids were removed by degassing the samples (60-80 mg), transferred in a pre-weighed glass, in a dynamic vacuum ($< 5\times10^{-3}$ mbar) at 298 K for at least 3 h before measurements. The specific surface area was determined-using the Langmuir and the Brunauer-Emmett-Teller (BET) calculations, and the pore volume were obtained directly from the N_2 adsorption/desorption isotherms at $P/P_0 = 0.99$. To avoid large discrepancies between the two values of the surface area due to the invalid BET assumption for microporous solids over the usual range $0.05 < P/P_0 < 0.25$, a suitable pressure range was applied, using a range that gives increasing values of $V_{N2}(P_0\text{-}P)$ with P/P_0, as required by the groups of Walton,[1] and Rouquerol.[2] Based on the consistency of this criteria, the pressure range used for the BET surface area calculations was then $0.01 < P/P_0 < 0.15$. The pore

size distribution of the materials was determined from the nitrogen adsorption isotherms using non-local density functional theory (NLDFT) using Saieus software.

Low-pressure gas adsorptions. Gas adsorption measurements for CO_2, N_2, and CO at 298 K were run on the Micromeritics ASAP 2020. The sample temperature was maintained using a Lauda cooler circulator and a double circulating jacket connected to a thermostatic bath in which the sample tube was dipped.

Experimental Procedures. Synthesis

Diethyl(4-formylphenyl)phosphonate[3]

In a round bottom flask equipped with an air condenser was introduced 4-bromobenzaldehyde (3.0 g, 16.2 mmol) and $Pd(PPh_3)_2Cl_2$ (340 mg, 10% mol.). After three cycles of vacuum/N_2, diethylphosphite (2.3 mL, 17.8 mmol), triethylamine ([0.7M], 24 mL) and toluene ([0.7M], 24 mL) were added. The mixture was stirred at 90 °C for 24 hours in an inert atmosphere, protected from light. The crude was extracted with chloroform (100 mL) and the organic phase was washed with distilled water (100 mL twice) and with a saturated NaCl solution (100 mL). The organic phase was dried using anhydrous Na_2SO_4, filtered and the solvent removed under vacuum. The crude product was purified by silica chromatography column with chloroform and ethyl acetate as eluent (7:3) to afford the final product in 63% yield (1.2 g). ^{1}H NMR (500 MHz, $CDCl_3$): δ (ppm) 9.98 (s, 1H), 7.93-7.83 (m, 4H), 4.16-3.91 (m, 4H), 1.23 (s, t, J = 7.0 Hz, 6H).^{31}P NMR (202 MHz, $CDCl_3$): δ (ppm) 16.24.

General procedure for the synthesis of corroles A_2B

Dipyrromethane (1.0 mmol) and aldehyde (0.5 mmol, 0.5 eq) were dissolved in 50 mL of methanol. Then, a solution of HCl (37%, 2.5 mL) in H_2O (50 mL) was added and the reaction mixture was stirred at room temperature for 3 hours, protected from light. The crude was extracted with chloroform (400 mL for 3.4 mmol of aldehyde), the organic phase was washed with distilled water (400 mL twice), dried using anhydrous Na_2SO_4 and filtered. Then, *p*-chloranil (1.5 equiv.) was added and the reaction mixture was stirred at room temperature overnight, protected from light. The solvent was removed under vacuum and the crude product was purified to afford the final product as purple powder.

5,15-(2,6-dichlorophenyl)-10-diethylphenylphosphonate corrole (1a). Corrole **1a** was synthesized according to the general procedure described for the synthesis of A_2B-corroles using 420 mg of diethyl(4-formylphenyl)phosphonate and 1.0 g of 5-(2,6-dichlorophenyl)-dipyrromethane.[4]

Purifications details: The crude product was purified on silica plug with dichloromethane and ethyl acetate as eluent (8:2) to afford the final corrole **1a** in 22% yield (300 mg). ^{1}H NMR (500 MHz, $CDCl_3$): δ (ppm) 8.95 (d, J = 4.0 Hz, 2H), 8.51 (m, 4H), 8.37 (d, J = 4.5 Hz, 2H), 8.28 (m, 2H), 8.15 (m, 2H), 7.76 (d, J = 8.2 Hz, 4H), 7.64 (m, 2H), 4.33 (m, 4H), 1.47 (t, J = 7.0 Hz, 6H). ^{31}P NMR (202 MHz, $CDCl_3$): δ (ppm) 19.37. UV-Vis (CH_2Cl_2): λ_{max} (nm) ($\boldsymbol{\varepsilon}$ x 10^3 L.mol^{-1}.cm^{-1}) 409 (11.2), 425 (9.9), 567 (1.9), 608 (1.2), 633 (0.6). LRMS (MALDI-TOF, CH_2Cl_2) $[M]^{+\cdot}$: 798.12 (exp.), 798.09 (calc.). HRMS $[M+H]^+$: 799.0962 (exp.), 799.0960 (calc.).

5,15-(2,3,5,6-tetrafluorophenyl)-10-diethylphenylphosphonate corrole (1b)

Corrole **1b** was synthesized according the general procedure described for the synthesis of A_2B-corroles using 538 mg of diethyl(4-formylphenyl)phosphonate and 1.34 g of 5-(2,3,5,6-tetrafluorophenyl)dipyrromethane.[5]

Purifications details: The crude product was purified on a silica plug with dichloromethane and ethyl acetate as eluent (8:2) to afford the final corrole **1b** in 31% yield (553 mg).

^{1}H NMR (500 MHz, DMSO-d_6): δ (ppm) 9.02 (d, J = 4.0 Hz, 2H), 8.56 (d, J = 4.5 Hz, 2H), 8.50 (d, J = 4.0 Hz, 2H), 8.34 (d, J = 4.5 Hz, 2H), 8.29-8.24 (m, 4H), 8.06 (dd, J = 8 Hz, 2H), 4.25 (q, J = 7.0 Hz, 4H), 1.40 (t, J = 7.0 Hz, 6H).^{1}H decoupled ^{31}P NMR (500 MHz, DMSO-d_6): δ (ppm) 9.02 (d, J = 4.0 Hz, 2H), 8.56 (d, J = 4.5 Hz, 2H), 8.50 (d, J = 4.0 Hz, 2H), 8.34 (d, J = 4.5 Hz, 2H), 8.27 (d, J = 8.0 Hz, 2H), 8.24 (m, 2H), 8.06 (d, J = 8.0 Hz, 2H), 4.25 (q, J = 7.0 Hz, 4H), 1.40 (t, J = 7.0 Hz, 6H). ^{31}P NMR (202 MHz, DMSO-d_6): δ (ppm) 18.92. ^{19}F NMR (470 MHz, DMSO-d_6): δ (ppm) -139.38 (m, 4F), -140.17 (m, 4F). UV-Vis (CH_2Cl_2): λ_{max} (nm) ($\boldsymbol{\varepsilon}$ x 10^3 L.mol^{-1}.cm^{-1}) 411 (53.6), 565 (8.3), 612 (8.3), 640 (10.1). LMRS (MALDI-TOF, CH_2Cl_2) $[M+H]^+$: 807.18 (exp), 807.17 (calc). HRMS $[M+H]^+$: 807.1769 (exp.), 807.1766 (calc.)

General procedure for the hydrolysis of corroles

An oven-dried Schlenk was charged with diethylphenylphosphonate corrole (1.0 mmol), and after three cycles of vaccum/N_2, bromotrimethylsilane (8 equiv.) and CH_2Cl_2 (20 mL) was added. The mixture was stirred at room temperature for 48 hours under inert atmosphere. Distilled water (3 mL for 0.1 mmol of corrole) was poured and the mixture is kept stirring with maintenance of nitrogen gas flow for 48 hours. Afterwards, the mixture was filtrated and the precipitate washed three times with distilled water before dissolution using MeOH. The resulting powder was washed with diethyl ether.

5,15-(2,6-dichlorophenyl)-10-(4-phenylphosphonic acid) corrole (2a)

Corrole **2a** was synthesized according the general procedure described for the hydrolysis of corroles using 100 mg of (**1a**) and 0.1 mL of bromotrimethylsilane.

No additional purification was needed to afford the final corrole **2a** in 91% yield (67.6 mg). ^{1}H NMR (500 MHz, MeOD): δ (ppm) 8.96 (d, J = 4.0 Hz, 2H), 8.47 (d, J = 4.5 Hz, 2H), 8.35 (d, J = 4.5 Hz, 2H), 8.28 (d, J = 4.0 Hz, 2H), 8.20 (m, 2H), 8.14 (m, 2H), 7.82 (d, J = 8.0 Hz, 4H), 7.73 (t, J = 8.0 Hz, 2H). ^{1}H NMR decoupled ^{31}P (500 MHz, MeOD): δ (ppm) 8.96 (d, J = 4.0 Hz, 2H), 8.47 (d, J = 4.5 Hz, 2H), 8.35 (d, J = 4.5 Hz, 2H), 8.28 (d, J = 4.0 Hz, 2H), 8.20 (d, J = 7.5 Hz, 2H), 8.14 (d, J = 7.5 Hz, 2H), 7.82 (d, J = 8.0 Hz, 4H), 7.73 (t, J = 8.0 Hz, 3H). ^{31}P NMR (202 MHz, MeOD): δ (ppm) 12.39. UV-Vis (MeOH): λ_{max} (nm) (**ε** x 10^{-3} L.mol^{-1}.cm^{-1}) 407 (83.3), 426 (63.5), 570 (15.9), 608 (9.93), 641 (3.97). LRMS (MALDI-TOF, THF) $[M]^{+\cdot}$: 742.06 (exp.), 742.03 (calc). HRMS $[M+H]^{+}$: 743.0327 (exp.), 743.0335 (calc.).

5,15-(2,3,5,6-tetrafluorophenyl)-10-(4-phenylphosphonic acid) corrole (2b)

Corrole **2b** was synthesized according the general procedure described for the hydrolysis of corroles using 100 mg of corrole **1b** and 0.14 mL of bromotrimethylsilane.

No additional purification was needed to afford the final corrole **2b** in 72% yield (67.8 mg). ^{1}H NMR (500 MHz, MeOD): δ (ppm) 9.50 (d, J = 4.5 Hz, 2H), 9.10 (d, J = 5.0 Hz, 2H), 8.92 (d, J = 4.5 Hz, 2H), 8.80 (d, J = 5.0 Hz, 2H), 8.54 (m, 2H), 8.35 (m, 2H), 8.07 (m, 2H). ^{1}H NMR decoupled ^{31}P (500 MHz, MeOD): δ (ppm) 9.50 (d, J = 4.5 Hz, 2H), 9.09 (d, J = 5.0 Hz, 2H), 8.91 (d, J = 4.5 Hz, 2H), 8.80 (d, J = 5.0 Hz, 2H), 8.54 (d, J = 7.5 Hz, 2H), 8.35 (d, J = 7.5 Hz, 2H), 8.06 (m, 2H). ^{19}F NMR (470 MHz, MeOD): δ (ppm) -140.47 (m, 4H), -142.10 (m, 4H). ^{31}P NMR (202 MHz, MeOD): δ (ppm) 15.21. UV-Vis (MeOH): λ_{max} (nm) (**ε** x 10^{-3} L.mol^{-1}.cm^{-1}) 418 (79.7), 597 (10.0), 611 (10.7), 645 (17.6). LCMS (MALDI-TOF, MeOH) $[M+H]^{+}$: 751.23 (exp.), 751.11 (calc.). HRMS $[M+H]^{+}$: 751.1134 (exp.), 751.1140 (calc.).

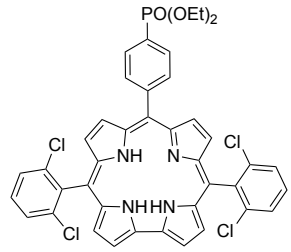

Chemical Formula: $C_{41}H_{31}Cl_4N_4O_3P$
Exact Mass: 798,09
Molecular Weight: 800,50

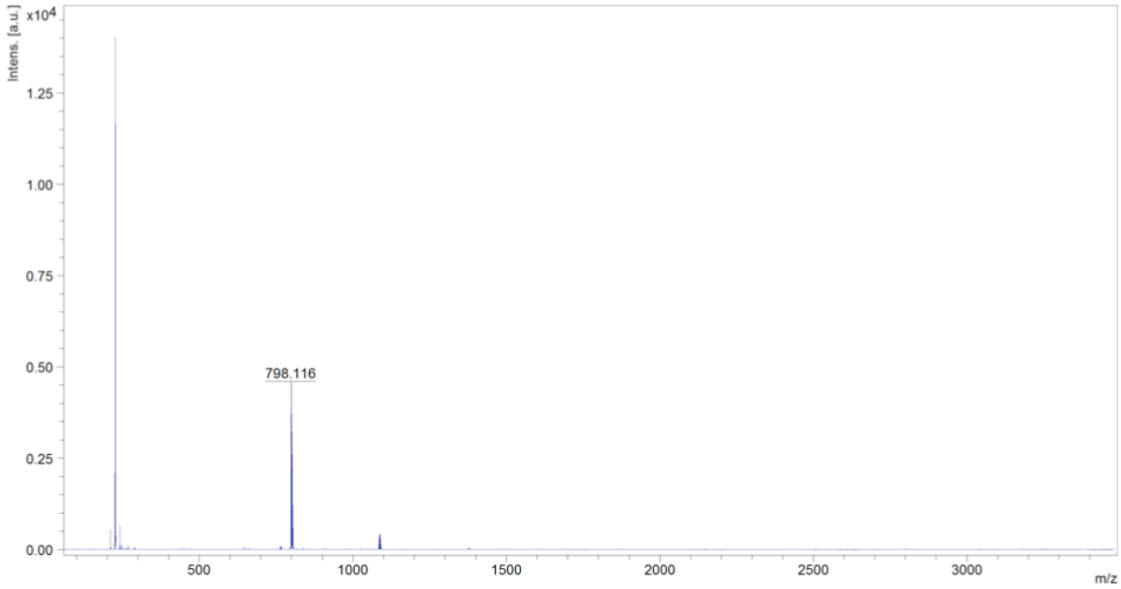

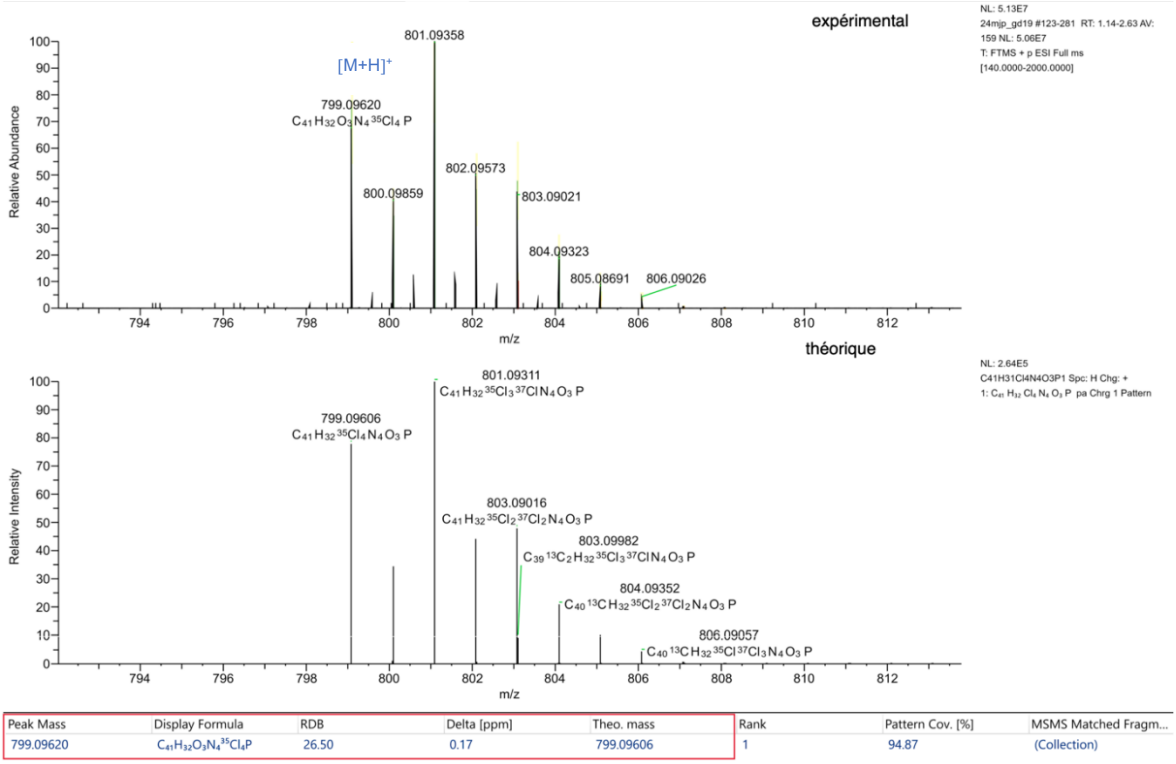

Peak Mass	Display Formula	RDB	Delta [ppm]	Theo. mass	Rank	Pattern Cov. [%]	MSMS Matched Fragm...
799.09620	$C_{41}H_{32}O_3N_4{}^{35}Cl_4P$	26.50	0.17	799.09606	1	94.87	(Collection)

Figure S1. LRMS (MALDI-TOF) and HRMS (ESI) spectra of corrole **1a**

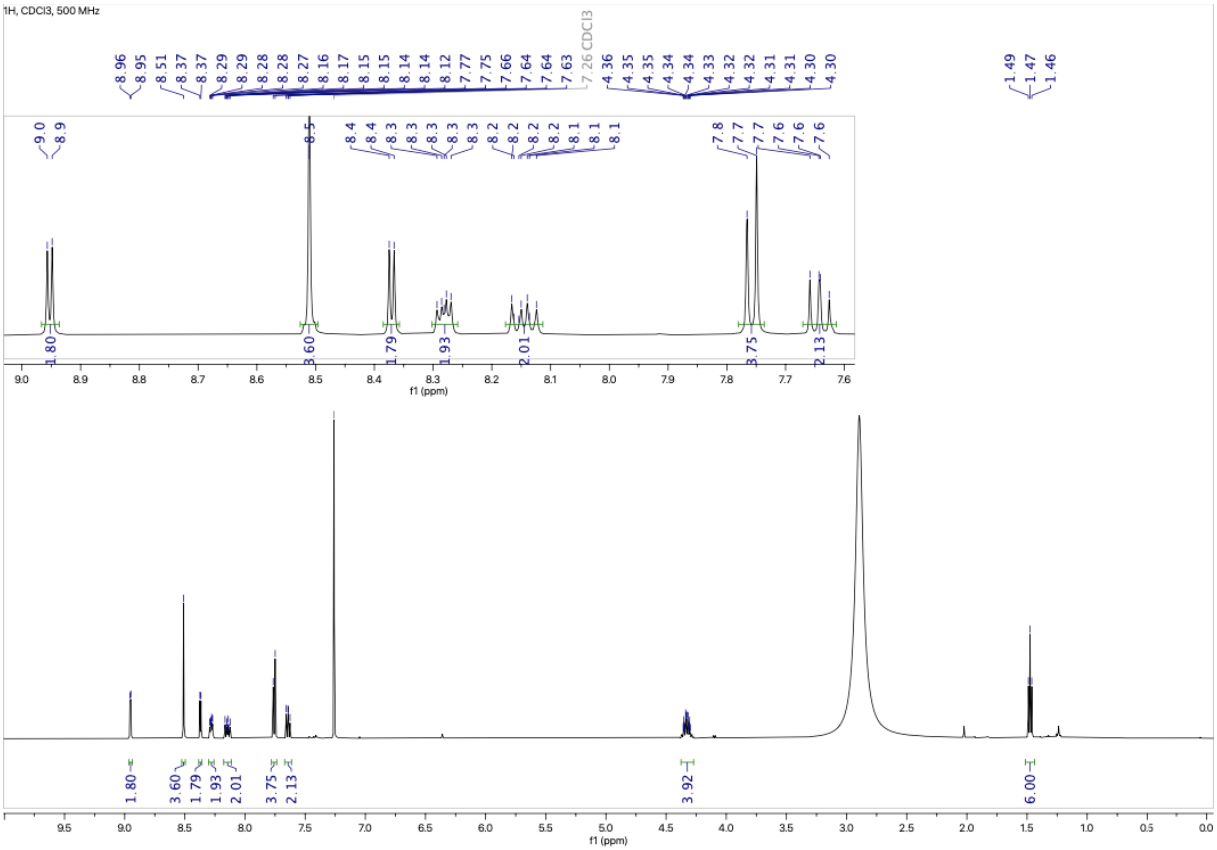

Figure S2. ^{1}H NMR spectrum (500 MHz, $CDCl_3$) of corrole **1a**

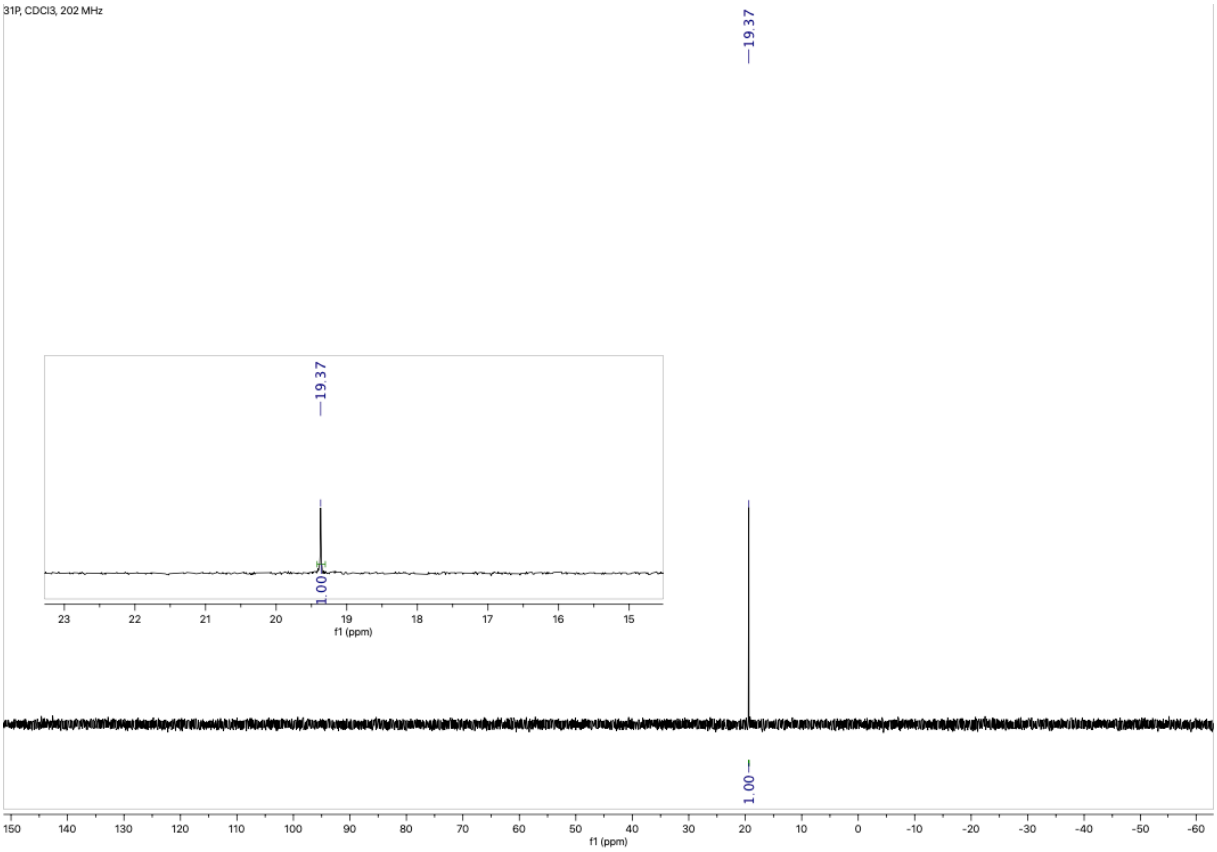

Figure S3. ^{31}P (^{1}H decoupled) NMR spectrum (202 MHz, $CDCl_3$) of corrole **1a**

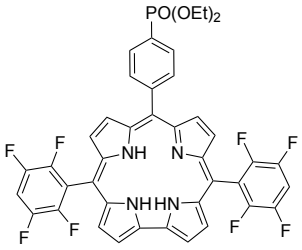

Chemical Formula: $C_{41}H_{27}F_8N_4O_3P$
Exact Mass: 806,17
Molecular Weight: 806,65

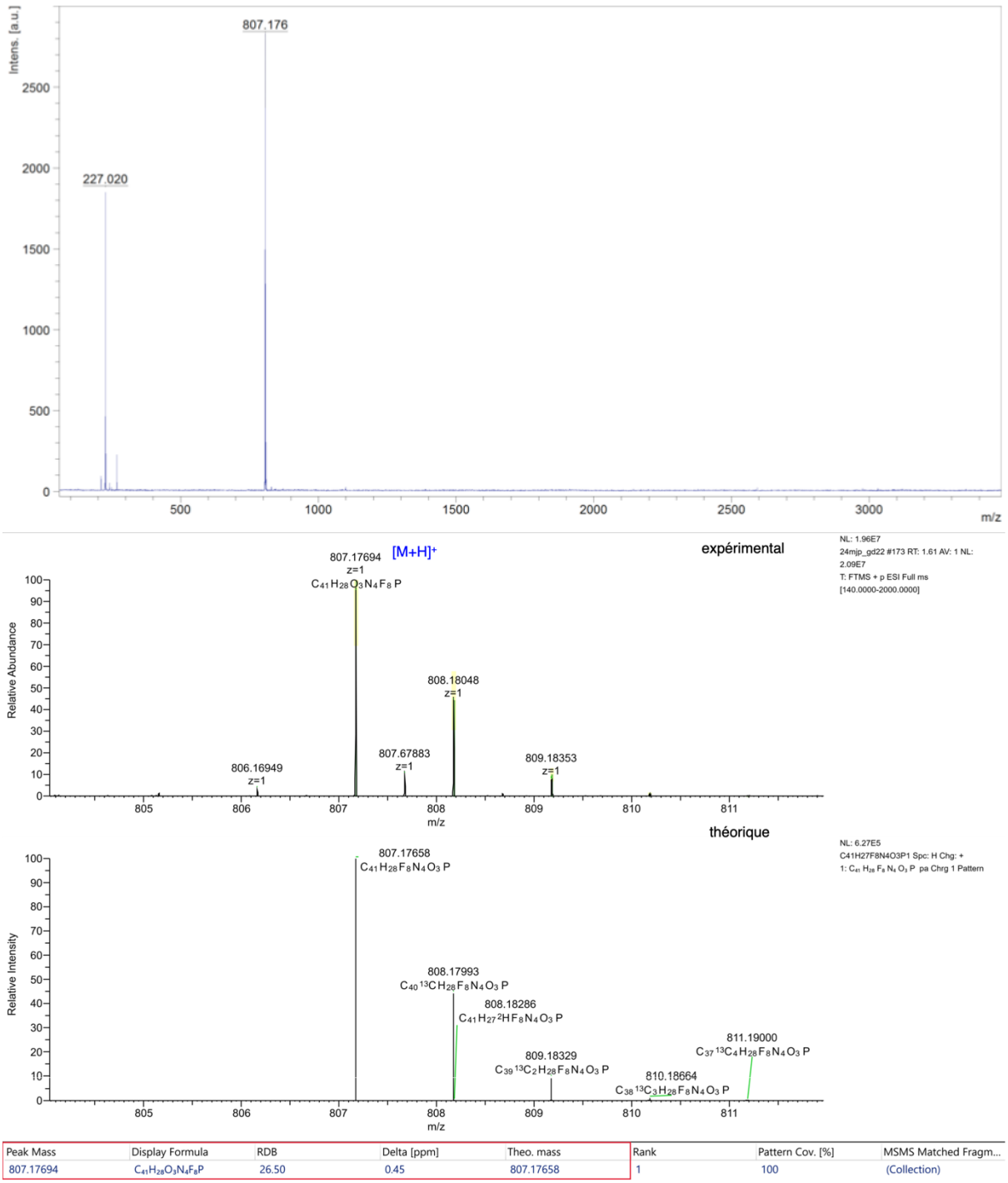

Peak Mass	Display Formula	RDB	Delta [ppm]	Theo. mass	Rank	Pattern Cov. [%]	MSMS Matched Fragm...
807.17694	$C_{41}H_{28}O_3N_4F_8P$	26.50	0.45	807.17658	1	100	(Collection)

Figure S4. LRMS (MALDI-TOF) and HRMS (ESI) spectra of corrole **1b**

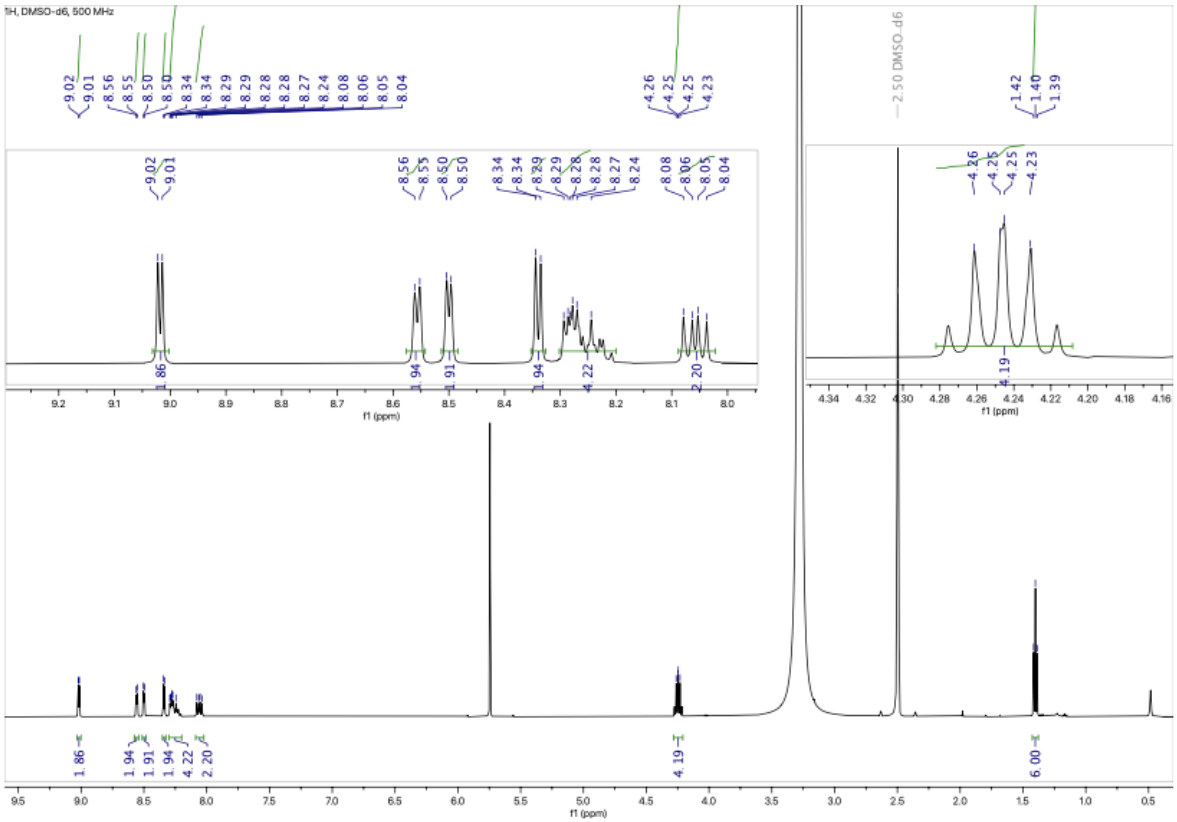

Figure S5. ^{1}H NMR spectrum (500 MHz, DMSO-d_6) of corrole **1b**

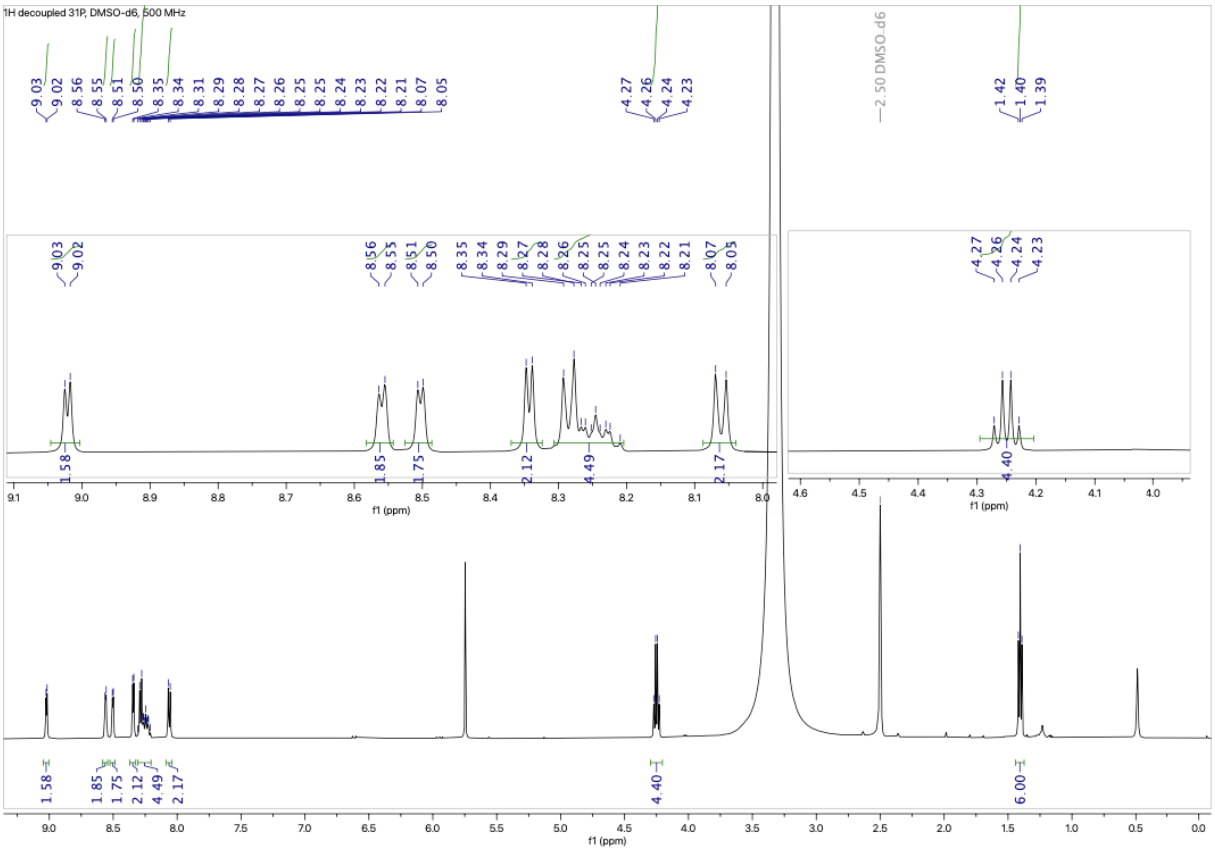

Figure S6. ^{1}H (^{31}P decoupled) NMR spectrum (500 MHz, DMSO-d_6) of corrole **1b**

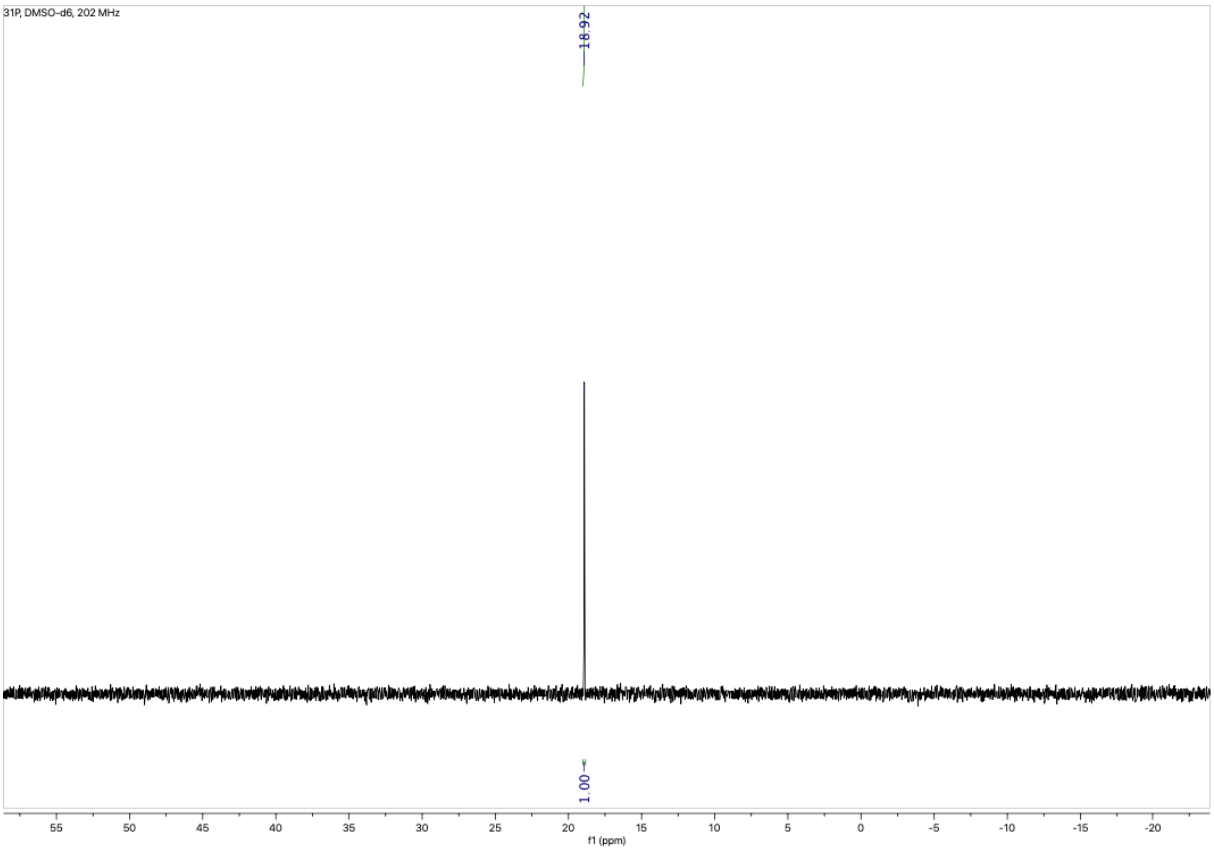

Figure S7. ^{31}P (^{1}H decoupled) NMR spectrum (202 MHz, DMSO-d_6) of corrole **1b**

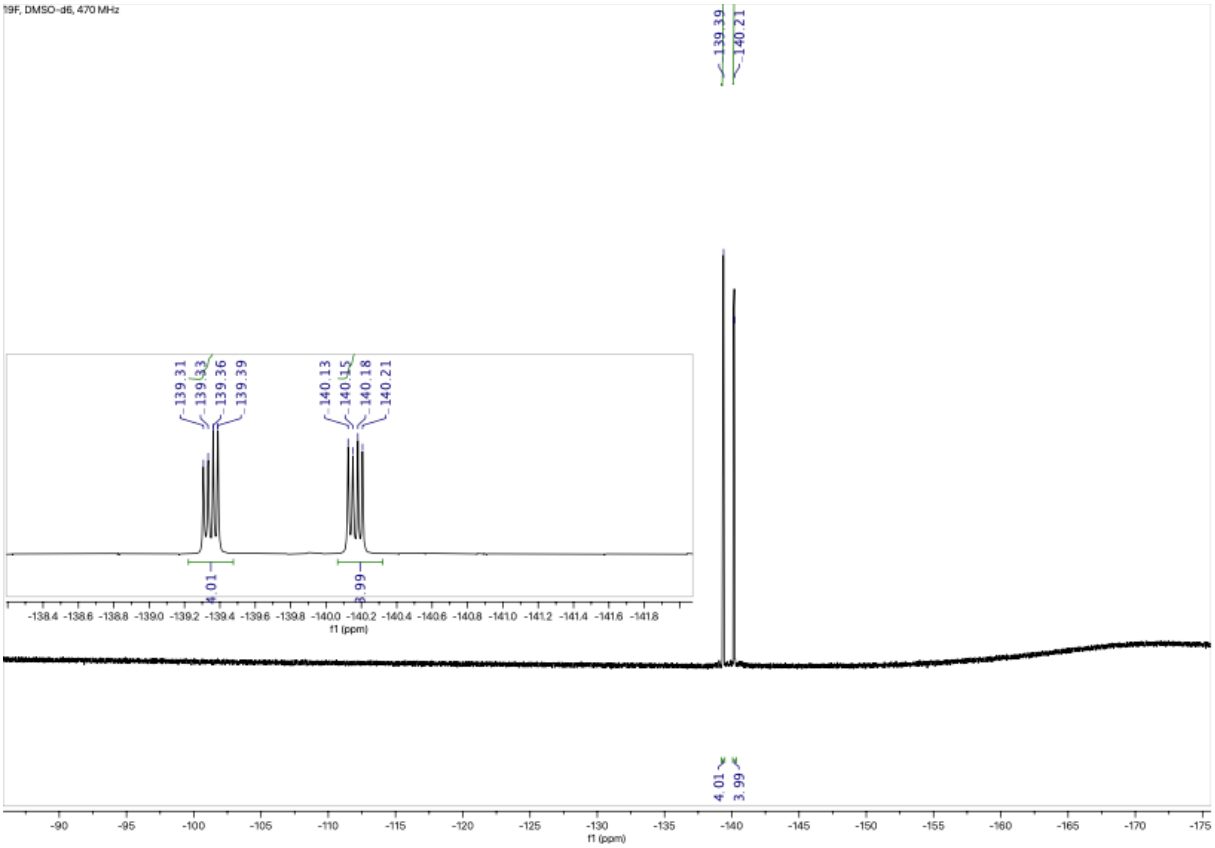

Figure S8. ^{19}F (^{1}H decoupled) NMR spectrum (470 MHz, DMSO-d_6) of corrole **1b**

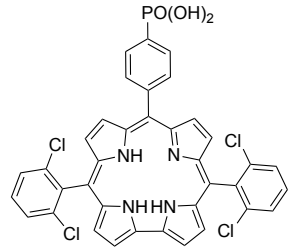

Chemical Formula: $C_{37}H_{23}Cl_4N_4O_3P$
Exact Mass: 742,03
Molecular Weight: 744,39

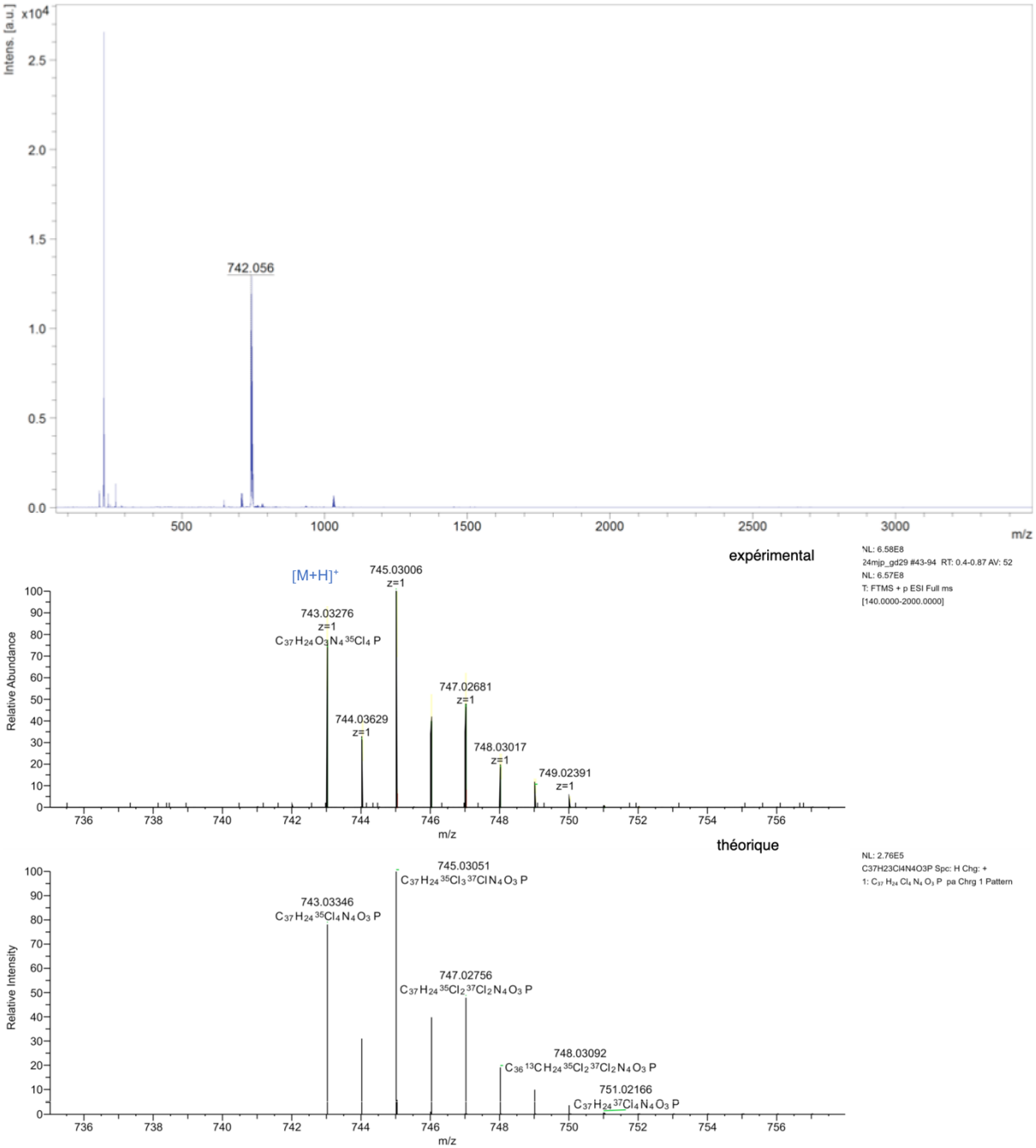

Peak Mass	Display Formula	RDB	Delta [ppm]	Theo. mass	Rank	Pattern Cov. [%]	MSMS Matched Fragm...
743.03276	$C_{37}H_{24}O_3N_4{}^{35}Cl_4P$	26.50	-0.95	743.03346	1	95.7	(Collection)

Figure S9. LRMS (MALDI-TOF) and HRMS (ESI) spectra of corrole **2a**

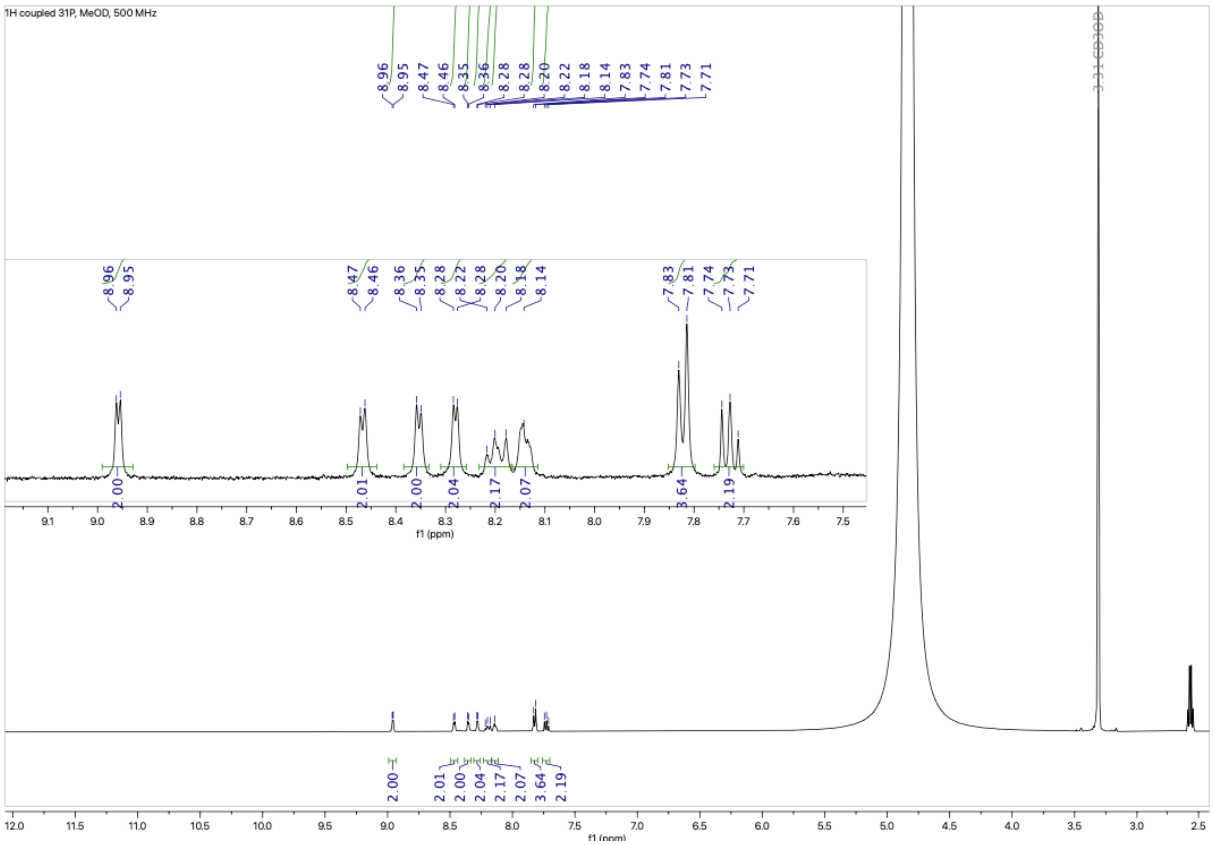

Figure S10. ^{1}H NMR spectrum (500 MHz, MeOD) of corrole **2a**

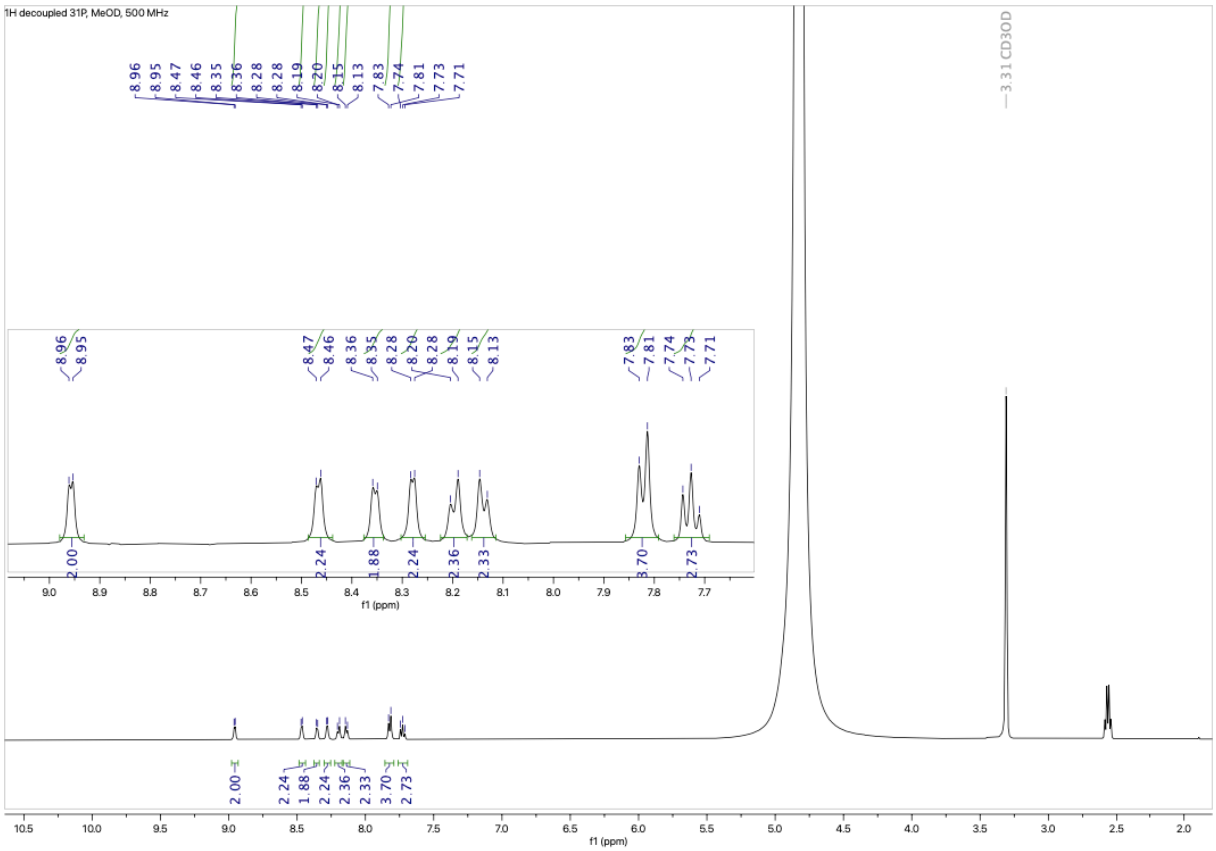

Figure S11. ^{1}H (^{31}P decoupled) NMR spectrum (500 MHz, MeOD) of corrole **2a**

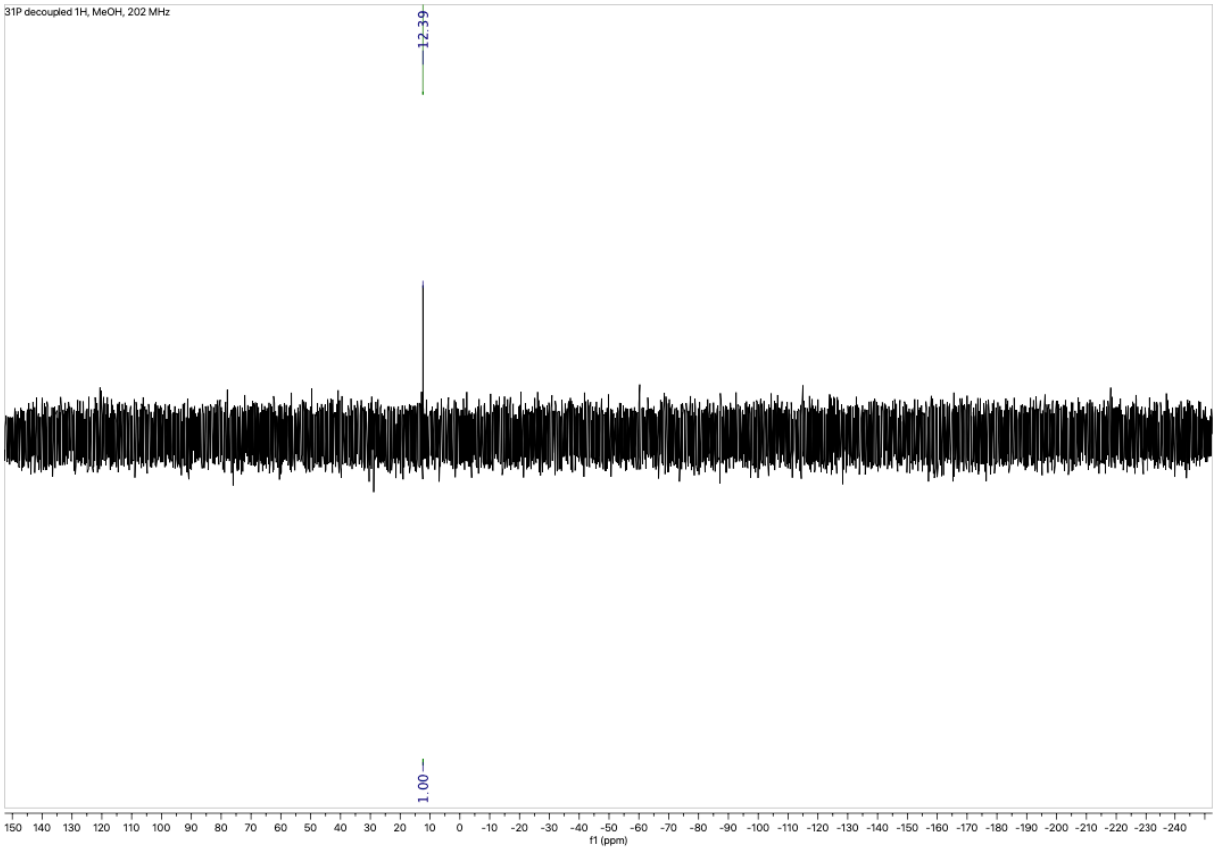

Figure S12. ^{31}P (^{1}H decoupled) NMR spectrum (202 MHz, MeOD) of corrole **2a**

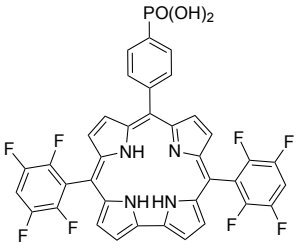

Chemical Formula: $C_{37}H_{19}F_8N_4O_3P$
Exact Mass: 750,11
Molecular Weight: 750,54

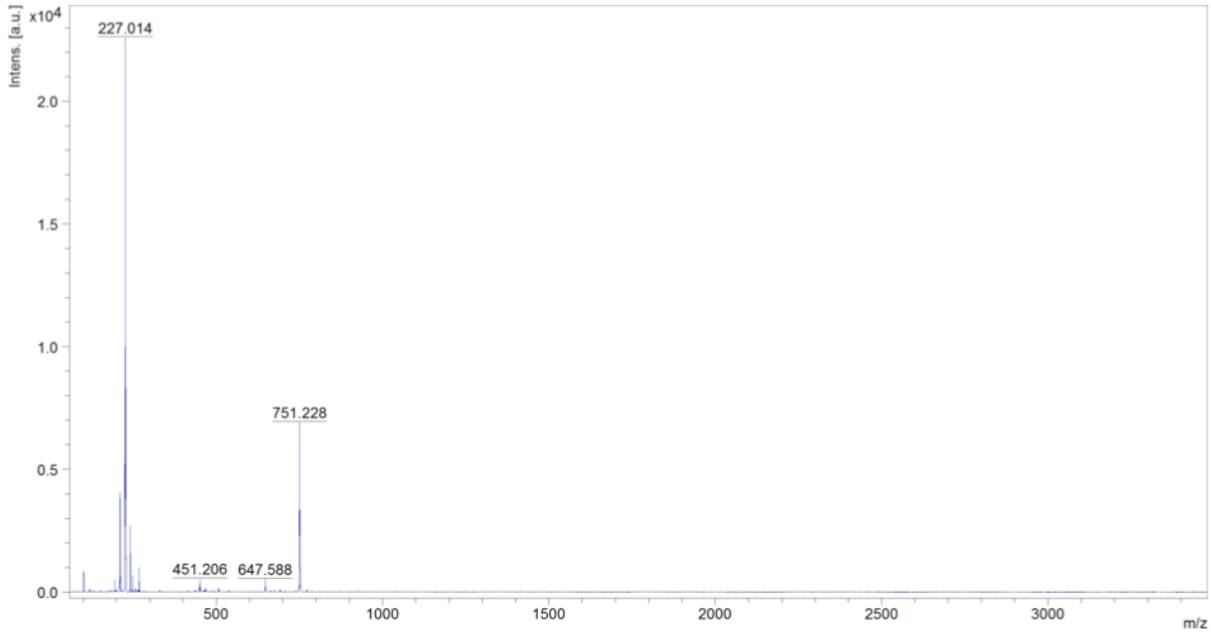

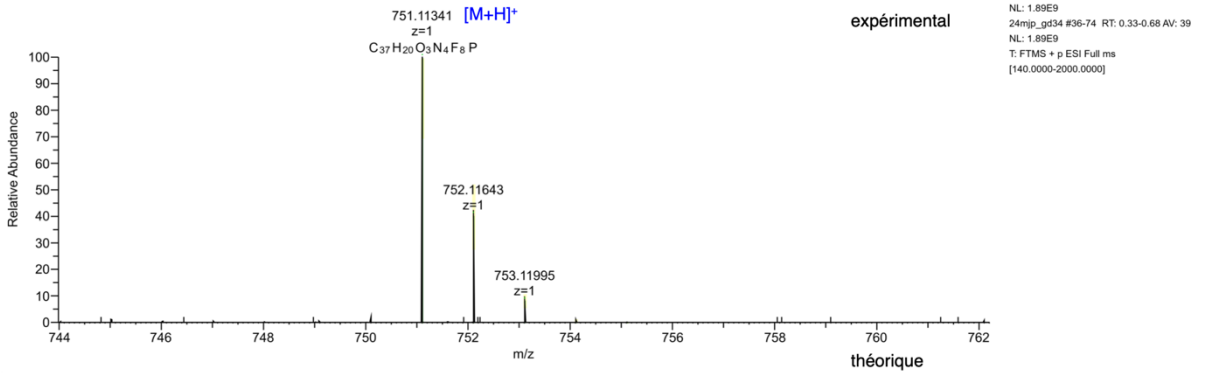

Peak Mass	Display Formula	RDB	Delta [ppm]	Theo. mass	Rank	Pattern Cov. [%]	MSMS Matched Fragm...
751.11341	$C_{37}H_{20}O_3N_4F_8P$	26.50	-0.76	751.11398	1	100	(Collection)

Figure S13. LRMS (MALDI-TOF) and HRMS (ESI) spectra of corrole **2b**

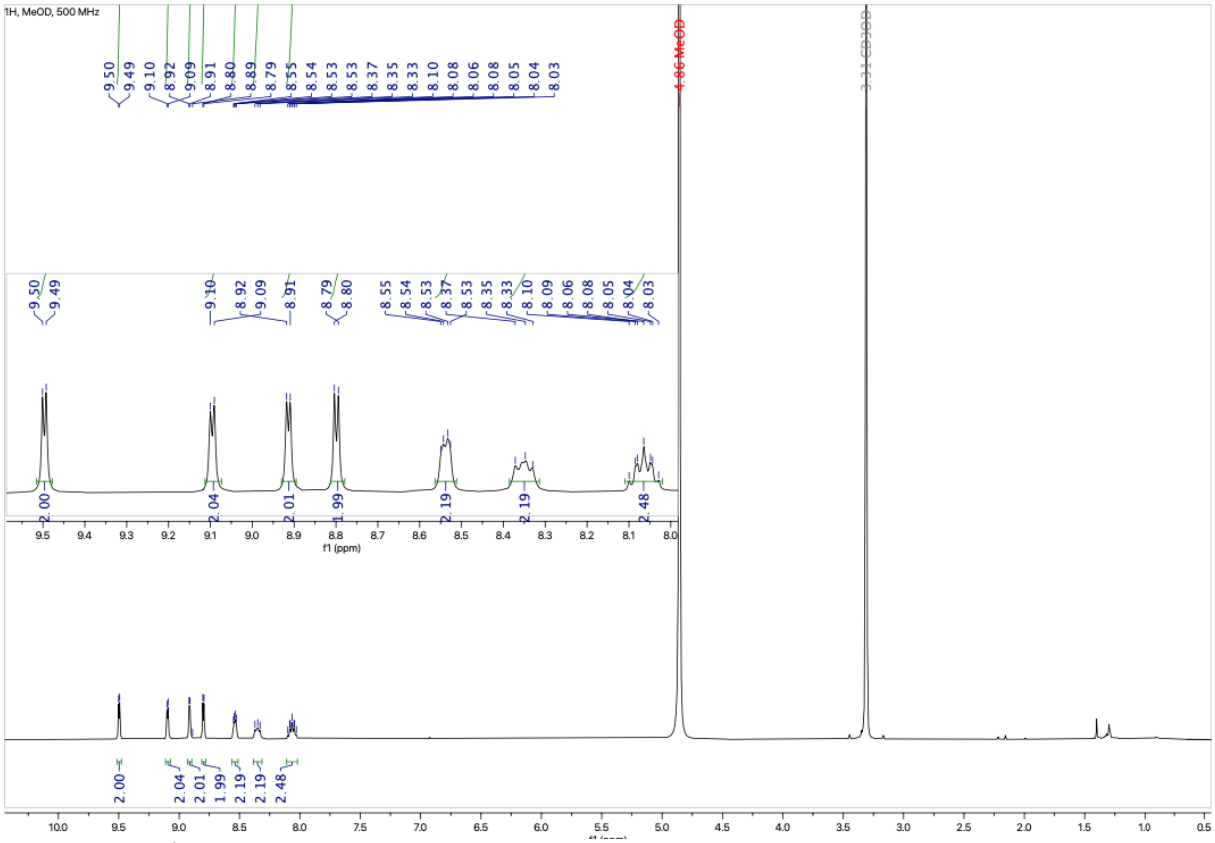

Figure S14. ^{1}H NMR spectrum (500 MHz, MeOD) of corrole **2b**

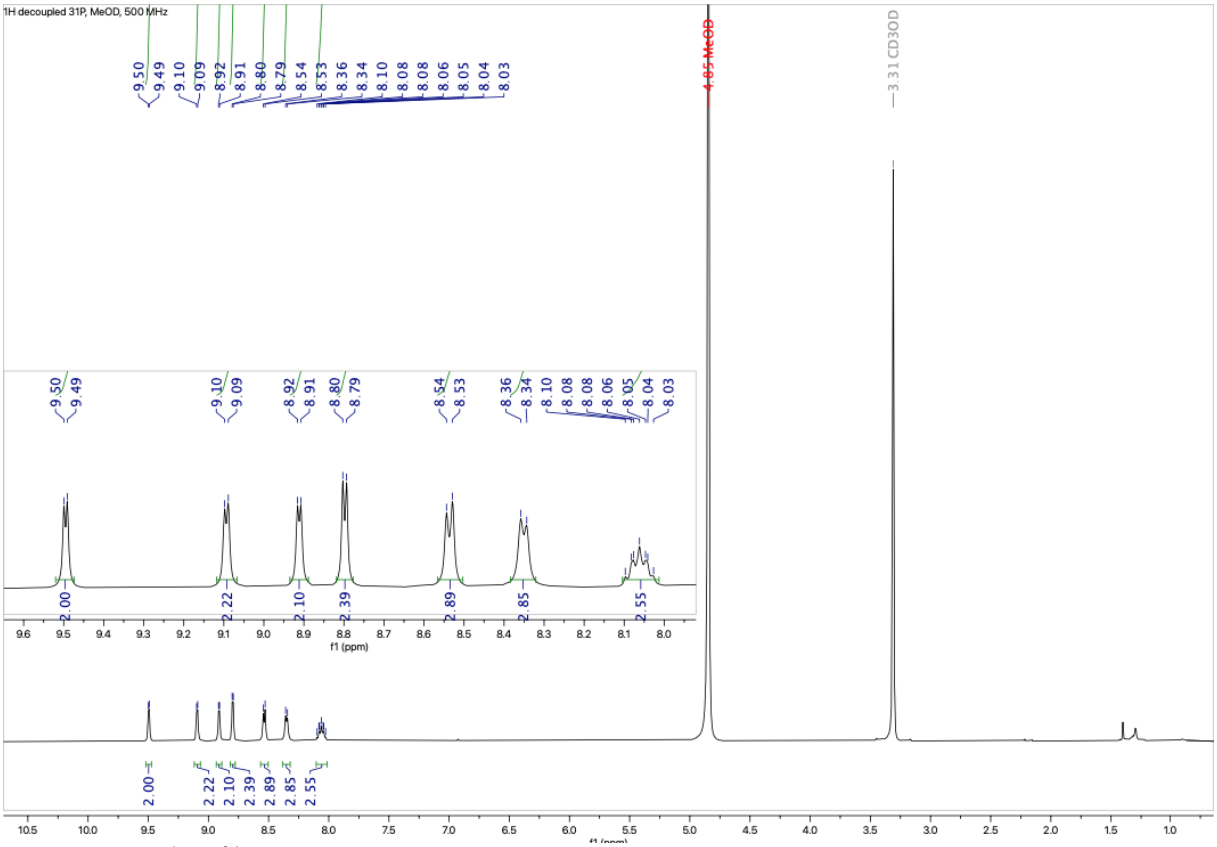

Figure S15. ^{1}H (^{31}P decoupled) NMR spectrum (500 MHz, MeOD) of corrole **2b**

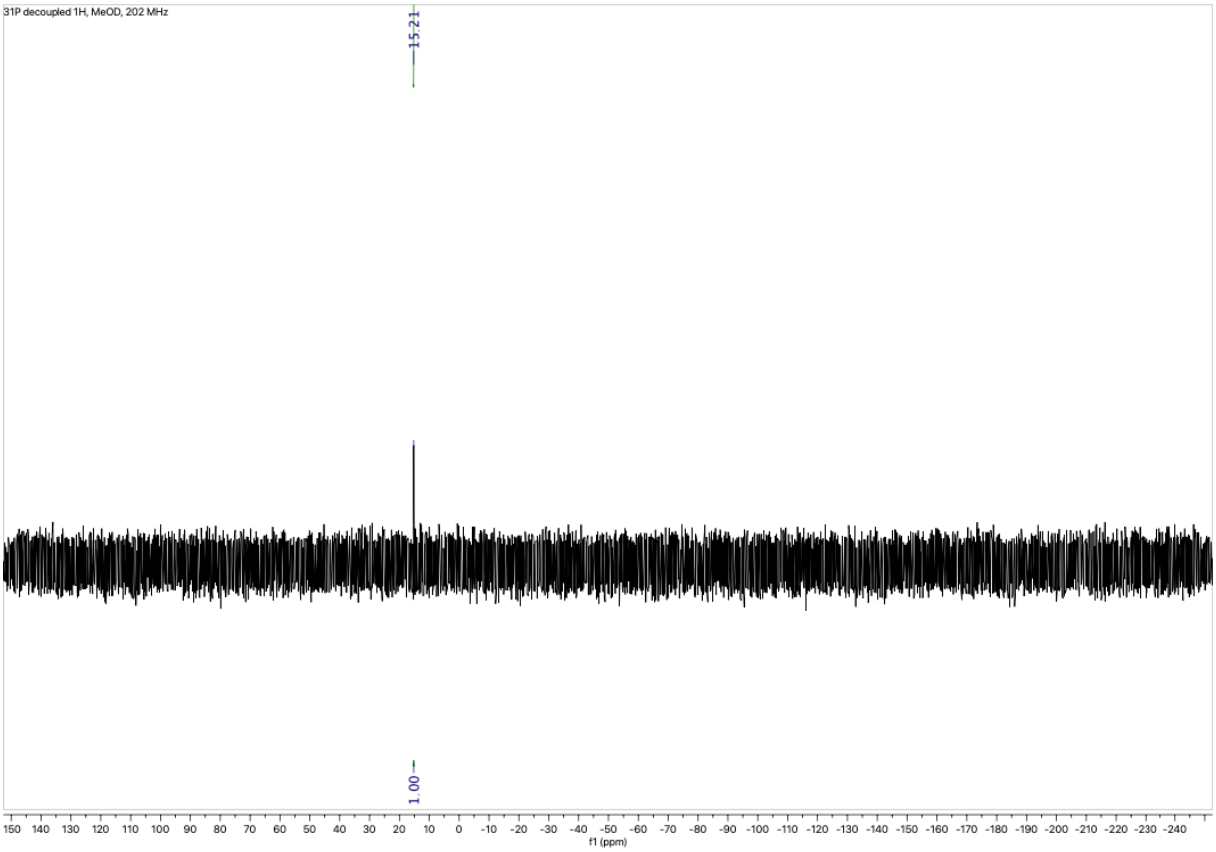

Figure S16. ^{31}P (^{1}H decoupled) NMR spectrum (202 MHz, MeOD) of corrole **2b**

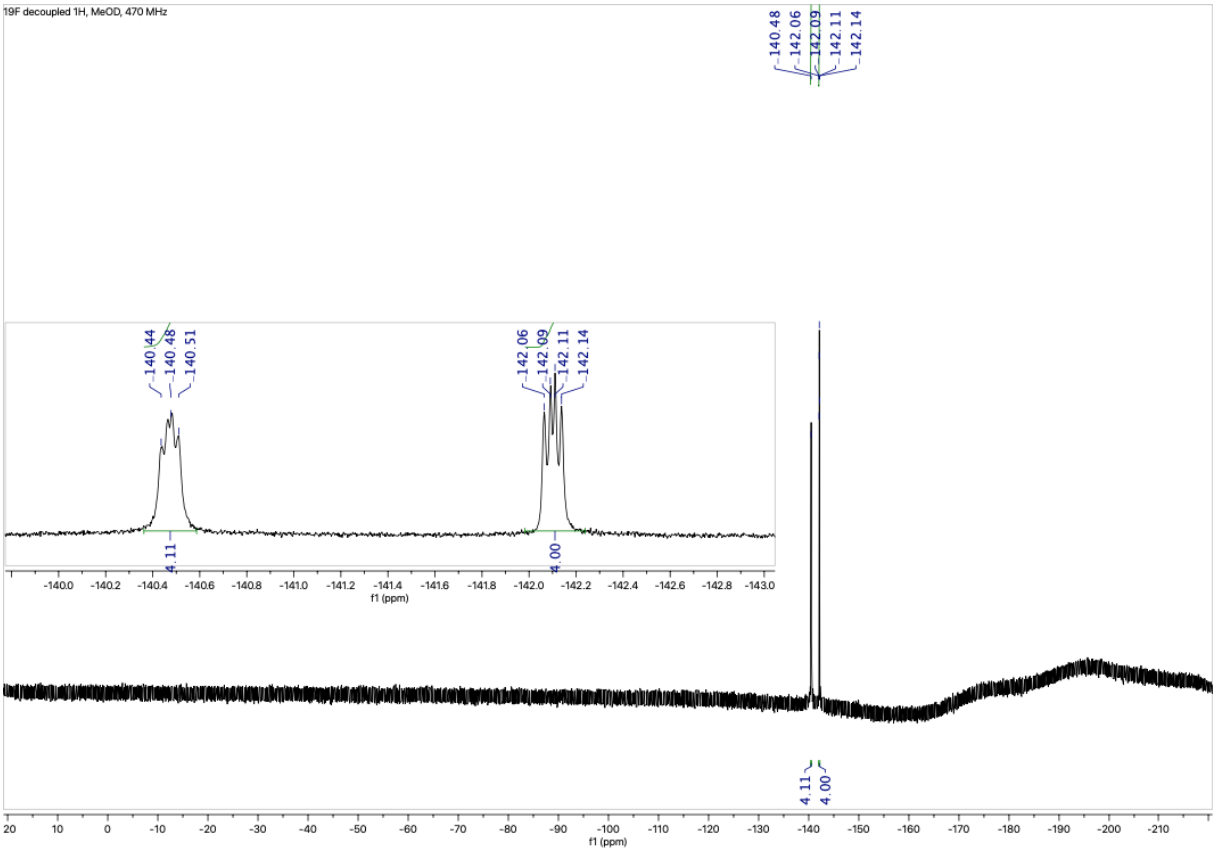

Figure S17. ^{19}F (^{1}H decoupled) NMR spectrum (470 MHz, DMSO-d^6) of corrole **2b**

Structure Tables for corrole 1b

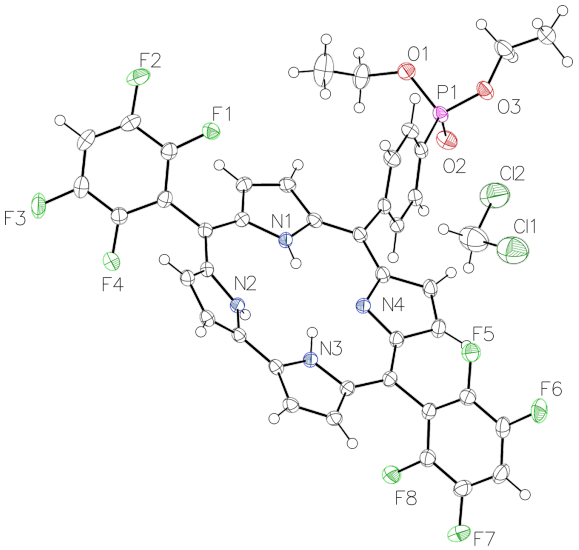

The material was recrystallized from DCM by slow diffusion of cyclohexane. A clear dark violet, prism-shaped crystal was mounted on a MiTeGen micromount with perfluoroether oil. Data for corrole **1b** were collected from a shock-cooled single crystal at 130(1) K on a Bruker D8 VENTURE dual wavelength Ag/Cu three-circle diffractometer with a microfocus sealed X-ray tube using a mirror optics as monochromator and a Bruker PHOTON III detector. The diffractometer was equipped with an Oxford Cryostream 800 low temperature device and used Cu K_α radiation (λ = 1.54178 Å). All data were integrated with SAINT V8.40B and a multi-scan absorption correction using SADABS 2016/2 was applied.[6,7] The structure was solved by dual methods with SHELXT and refined by full-matrix least-squares methods against F^2 using SHELXL.[8,9] All non-hydrogen atoms were refined with anisotropic displacement parameters. All C-bound hydrogen atoms were refined isotropic on calculated positions using a riding model with their U_{iso} values constrained to 1.5 times the U_{eq} of their pivot atoms for terminal sp^3 carbon atoms and 1.2 times for all other carbon atoms. Crystallographic data for the structures reported in this paper have been deposited with the Cambridge Crystallographic Data Centre.[10] CCDC 2395038 contain the supplementary crystallographic data for this paper. These data can be obtained free of charge from The Cambridge Crystallographic Data Centre via www.ccdc.cam.ac.uk/structures. This report and the CIF file were generated using FinalCif.[11]

Table S1. Crystal data and structure refinement for corrole **1b**

CCDC number	2395038
Internal reference	23GD22
Empirical formula	$C_{42}H_{29}Cl_2F_8N_4O_3P$
Formula weight	891.56
Temperature [K]	130(1)
Crystal system	triclinic
Space group (number)	$P\overline{1}$ (2)
a [Å]	10.9650(4)
b [Å]	13.7874(5)
c [Å]	15.5996(5)
α [°]	64.2197(15)
β [°]	73.4957(16)
γ [°]	67.1373(16)
Volume [Å^3]	1937.85(12)
Z	2
ρ_{calc} [gcm^{-3}]	1.528
μ [mm^{-1}]	2.657
F(000)	908
Crystal size [mm^3]	0.128×0.201×0.336
Crystal colour	clear dark violet
Crystal shape	prism
Radiation	Cu K_α (λ=1.54178 Å)
2θ range [°]	6.35 to 133.24 (0.84 Å)
Index ranges	−13 ≤ h ≤ 13 −16 ≤ k ≤ 16 −18 ≤ l ≤ 18
Reflections collected	105851
Independent reflections	6852 R_{int} = 0.0338 R_{sigma} = 0.0168
Completeness to θ = 66.620°	99.9
Data / Restraints / Parameters	6852 / 0 / 543
Absorption correction T_{min}/T_{max} (method)	0.5118 / 0.6285 (multi-scan)
Goodness-of-fit on F^2	1.033
Final *R* indexes [$I \geq 2\sigma(I)$]	R_1 = 0.0420 wR_2 = 0.1205
Final *R* indexes [all data]	R_1 = 0.0435 wR_2 = 0.1218
Largest peak/hole [eÅ^{-3}]	0.48/−0.71

Table S2. Bond lengths and angles for corrole **1b**

Atom–Atom	**Length [Å]**
Cl1–C42	1.754(4)
Cl2–C42	1.754(3)
C42–H42A	0.9900
C42–H42B	0.9900
P1–O1	1.5783(15)
P1–O2	1.4707(16)
P1–O3	1.5746(14)
P1–C23	1.7805(19)
F1–C31	1.341(2)
F2–C32	1.349(3)
F3–C34	1.347(3)
F4–C35	1.344(2)
F5–C37	1.345(2)
F6–C38	1.341(3)
F7–C40	1.350(3)
F8–C41	1.345(2)
O1–C26	1.460(3)
O3–C28	1.455(3)
N1–H1	0.9592
N1–C2	1.372(2)
N1–C5	1.386(2)
N2–H2	0.9280
N2–C7	1.377(2)
N2–C10	1.381(2)
N3–H3	0.9320
N3–C11	1.363(2)
N3–C14	1.362(2)
N4–C16	1.384(2)
N4–C19	1.364(2)
C1–C2	1.405(3)
C1–C19	1.421(3)
C1–C20	1.493(3)
C2–C3	1.435(3)
C3–H3A	0.9500
C3–C4	1.363(3)
C4–H4	0.9500
C4–C5	1.427(3)
C5–C6	1.404(3)
C6–C7	1.419(3)
C6–C30	1.481(3)
C7–C8	1.408(3)
C8–H8	0.9500
C8–C9	1.393(3)
C9–H9	0.9500
C9–C10	1.406(3)
C10–C11	1.413(3)
C11–C12	1.416(3)
C12–H12	0.9500
C12–C13	1.383(3)
C13–H13	0.9500
C13–C14	1.417(3)
C14–C15	1.410(3)
C15–C16	1.412(3)
C15–C36	1.493(3)
C16–C17	1.446(3)
C17–H17	0.9500
C17–C18	1.351(3)
C18–H18	0.9500
C18–C19	1.453(3)
C20–C21	1.399(3)
C20–C25	1.394(3)
C21–H21	0.9500
C21–C22	1.384(3)
C22–H22	0.9500
C22–C23	1.399(3)
C23–C24	1.390(3)
C24–H24	0.9500
C24–C25	1.390(3)
C25–H25	0.9500
C26–H26A	0.9900
C26–H26B	0.9900
C26–C27	1.465(4)
C27–H27A	0.9800
C27–H27B	0.9800
C27–H27C	0.9800
C28–H28A	0.9900
C28–H28B	0.9900
C28–C29	1.483(3)
C29–H29A	0.9800
C29–H29B	0.9800
C29–H29C	0.9800
C30–C31	1.397(3)
C30–C35	1.399(3)
C31–C32	1.383(3)
C32–C33	1.376(3)
C33–H33	0.9500
C33–C34	1.371(3)
C34–C35	1.382(3)
C36–C37	1.386(3)
C36–C41	1.394(3)
C37–C38	1.382(3)
C38–C39	1.380(3)
C39–H39	0.9500
C39–C40	1.377(3)
C40–C41	1.380(3)
Atom–Atom–Atom	**Angle [°]**
Cl1–C42–Cl2	111.6(2)
Cl1–C42–H42A	109.3
Cl1–C42–H42B	109.3
Cl2–C42–H42A	109.3
Cl2–C42–H42B	109.3
H42A–C42–H42B	108.0
O1–P1–C23	107.55(9)
O2–P1–O1	115.03(8)
O2–P1–O3	116.19(9)
O2–P1–C23	112.95(9)
O3–P1–O1	100.89(8)
O3–P1–C23	102.82(8)

C26–O1–P1	119.86(14)
C28–O3–P1	119.43(14)
C2–N1–H1	122.4
C2–N1–C5	111.80(15)
C5–N1–H1	125.5
C7–N2–H2	122.8
C7–N2–C10	110.14(15)
C10–N2–H2	122.2
C11–N3–H3	122.3
C14–N3–H3	123.3
C14–N3–C11	111.42(16)
C19–N4–C16	106.41(15)
C2–C1–C19	126.16(17)
C2–C1–C20	114.80(16)
C19–C1–C20	118.94(17)
N1–C2–C1	125.95(17)
N1–C2–C3	105.34(16)
C1–C2–C3	128.59(17)
C2–C3–H3A	125.6
C4–C3–C2	108.78(17)
C4–C3–H3A	125.6
C3–C4–H4	125.6
C3–C4–C5	108.74(17)
C5–C4–H4	125.6
N1–C5–C4	105.33(16)
N1–C5–C6	125.68(17)
C6–C5–C4	128.96(18)
C5–C6–C7	122.09(17)
C5–C6–C30	119.81(17)
C7–C6–C30	117.92(17)
N2–C7–C6	120.04(17)
N2–C7–C8	106.87(16)
C8–C7–C6	132.50(18)
C7–C8–H8	126.0
C9–C8–C7	108.05(17)
C9–C8–H8	126.0
C8–C9–H9	126.1
C8–C9–C10	107.88(16)
C10–C9–H9	126.1
N2–C10–C9	107.00(16)
N2–C10–C11	115.67(16)
C9–C10–C11	135.69(17)
N3–C11–C10	116.37(16)
N3–C11–C12	106.54(16)
C10–C11–C12	136.84(18)
C11–C12–H12	126.2
C13–C12–C11	107.60(17)
C13–C12–H12	126.2
C12–C13–H13	125.9
C12–C13–C14	108.12(16)
C14–C13–H13	125.9
N3–C14–C13	106.13(16)
N3–C14–C15	119.23(17)
C15–C14–C13	133.80(17)
C14–C15–C16	122.82(17)
C14–C15–C36	116.55(16)
C16–C15–C36	120.46(17)
N4–C16–C15	124.31(17)

N4–C16–C17	109.74(16)
C15–C16–C17	125.92(18)
C16–C17–H17	126.6
C18–C17–C16	106.87(17)
C18–C17–H17	126.6
C17–C18–H18	126.4
C17–C18–C19	107.21(17)
C19–C18–H18	126.4
N4–C19–C1	125.11(17)
N4–C19–C18	109.77(16)
C1–C19–C18	125.11(17)
C21–C20–C1	120.55(17)
C25–C20–C1	120.44(17)
C25–C20–C21	118.88(17)
C20–C21–H21	119.7
C22–C21–C20	120.68(18)
C22–C21–H21	119.7
C21–C22–H22	120.0
C21–C22–C23	119.91(18)
C23–C22–H22	120.0
C22–C23–P1	120.71(15)
C24–C23–P1	119.47(15)
C24–C23–C22	119.78(17)
C23–C24–H24	120.0
C23–C24–C25	119.99(18)
C25–C24–H24	120.0
C20–C25–H25	119.7
C24–C25–C20	120.67(18)
C24–C25–H25	119.7
O1–C26–H26A	109.5
O1–C26–H26B	109.5
O1–C26–C27	110.7(2)
H26A–C26–H26B	108.1
C27–C26–H26A	109.5
C27–C26–H26B	109.5
C26–C27–H27A	109.5
C26–C27–H27B	109.5
C26–C27–H27C	109.5
H27A–C27–H27B	109.5
H27A–C27–H27C	109.5
H27B–C27–H27C	109.5
O3–C28–H28A	110.0
O3–C28–H28B	110.0
O3–C28–C29	108.2(2)
H28A–C28–H28B	108.4
C29–C28–H28A	110.0
C29–C28–H28B	110.0
C28–C29–H29A	109.5
C28–C29–H29B	109.5
C28–C29–H29C	109.5
H29A–C29–H29B	109.5
H29A–C29–H29C	109.5
H29B–C29–H29C	109.5
C31–C30–C6	122.89(18)
C31–C30–C35	115.31(18)
C35–C30–C6	121.75(18)
F1–C31–C30	120.66(17)
F1–C31–C32	117.42(18)

C32–C31–C30	121.89(19)
F2–C32–C31	117.6(2)
F2–C32–C33	120.53(19)
C33–C32–C31	121.9(2)
C32–C33–H33	121.5
C34–C33–C32	117.06(19)
C34–C33–H33	121.5
F3–C34–C33	119.91(19)
F3–C34–C35	118.2(2)
C33–C34–C35	121.8(2)
F4–C35–C30	119.77(18)
F4–C35–C34	118.18(18)
C34–C35–C30	122.03(19)
C37–C36–C15	121.74(18)
C37–C36–C41	115.97(17)
C41–C36–C15	122.16(17)

F5–C37–C36	119.80(17)
F5–C37–C38	118.18(18)
C38–C37–C36	122.00(19)
F6–C38–C37	118.3(2)
F6–C38–C39	120.26(19)
C39–C38–C37	121.4(2)
C38–C39–H39	121.4
C40–C39–C38	117.22(19)
C40–C39–H39	121.4
F7–C40–C39	119.87(19)
F7–C40–C41	118.6(2)
C39–C40–C41	121.6(2)
F8–C41–C36	119.84(17)
F8–C41–C40	118.32(19)
C40–C41–C36	121.84(19)

Table 3. Hydrogen bonds for corrole **1b**

D–H···A [Å]	**d(D–H) [Å]**	**d(H···A) [Å]**	**d(D···A) [Å]**	**<(DHA) [°]**
N1–H1···N4	0.96	2.34	2.935(2)	119.8
N2–H2···O2$^{\#1}$	0.93	1.93	2.812(2)	158.6
N3–H3···N4	0.93	1.93	2.634(2)	130.7

Symmetry transformations used to generate equivalent atoms:
#1: 1-X, 2-Y, 1-Z;

Synthesis of PCN-222

In a round bottom flask (RBF), NiTCPP (0.7 mmol, 1 eq)[12] and zirconium dichloride oxide (6 mmol, 9 eq) were dissolved in 90 mL of DMF under magnetic stirring at room temperature. Dichloroacetic acid (DAA) (200 mmol, 300 eq) was then slowly added to the mixture, and the solution was kept under stirring for 1 h. The magnetic stirring was then stopped, the magnetic stirrer removed, and the solution was heated at 120 °C in a closed RBF for 48 h. After cooling to room temperature, the crystalline powder was washed three times with DMF and three times with acetone (about 3 x 15 mL). PCN-222 was obtained as a red crystalline powder and was kept in acetone until further use.

The following step was the activation of the synthesized PCN-222 to remove the modulator and free the vacancies for further addition of corrole inside the MOF. The MOF was activated with a solution of 0.1 M HCl in acetone for 3 h (2 washings of 1.5 h to renew the HCl bath). Then the activated PCN-222 was washed three times with acetone to remove HCl, and the material was dried under vacuum at room temperature before the corrole grafting step. The ^{1}H NMR analysis of PCN-222 after digestion in DMSO-d_6/DCl/NaF was conducted on the as-synthesized material and after the acidic activation in order to identify the presence of the modulator, dichloroacetic acid, and then to confirm its complete removal from the structure.

Corroles grafted inside activated PCN-222

In a general procedure, the corrole (0.16 mmol, 2 eq) to be grafted was dissolved in 5 mL of DMF using an ultra-sonic bath and poured in a 20 mL Pyrex tube. Then the activated PCN-222 (100 mg, 0.08 mmol, 1 eq) was added to the solution with 5 mL of DMF. The closed tube was heated at 60 °C in an oven for 48 h. After cooling at room temperature, the powder was washed three times with DMF and three times with acetone. The modified PCN-222 was obtained as a dark red/brown crystalline powder and kept in acetone. The ratio of corrole *vs* porphyrin inside the PCN-222 was determined by ^{1}H NMR spectroscopy. The material was dissolved in a mixture of DMSO-d_6 with a very small amount of NaF and DCl in D_2O. Then, the amount of released porphyrin and corrole was further determined by ^{1}H NMR to determine their ratio (Figure S18).

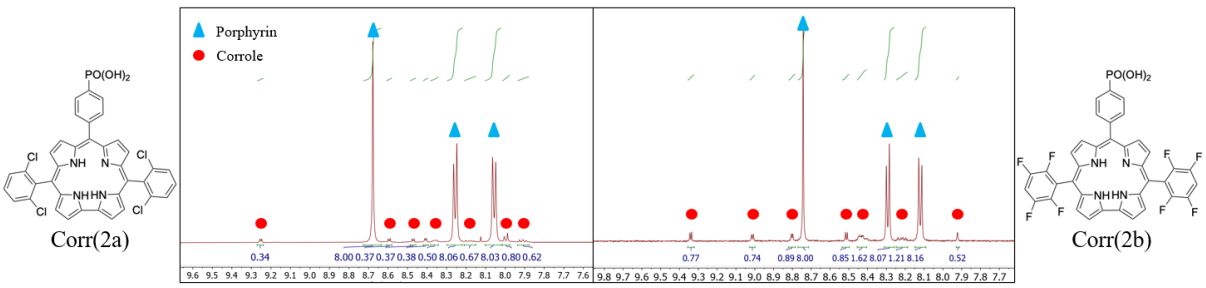

Figure S18. ^{1}H NMR spectra (500 MHz) of the two digested materials.

Grafted corroles cobalt metalation

In a general procedure, $Co(acac)_2$ (2 eq) was dissolved in 2 mL of anhydrous THF in a 20 mL Pyrex tube. **Corr@PCN-222** (1 eq) was added to the tube with 8 mL of DMSO (the final solution has an 8:2 ratio of DMSO:THF). The closed tube was heated at 80 °C for 48 h in an oven. The obtained material was washed once with a 8:2 DMSO: dry THF solution and three times with anhydrous THF to remove the excess of cobalt salt and DMSO. The resulting material was obtained as a dark red/brown crystalline powder and store in anhydrous THF before further analyses. Cobalt corroles grafted in PCN-222 are then stabilized by at least one DMSO ligand on the cobalt center.

Cobalt corroles activation

After metalation of grafted corroles, the material was dried under vacuum for 12 h at room temperature and put in an anhydrous THF solution saturated with NH_3 (NH_3:THF) at room temperature for 2 h, and the THF saturated with NH_3 bath was renewed once during that time. This is meant to replace the ligand DMSO on the cobalt center by NH_3. Indeed, by doing so, we were then able to activate the cobalt center (remove the ligand) more easily as NH_3 can be removed simply by heating at 80 °C under vacuum. Afterwards, the material was washed three times with anhydrous THF to remove the excess of NH_3. The final material containing the active species was obtained by drying under vacuum at 80 °C for few hours for gas adsorption measurements.

Table S5. Experimental ICP and elementary analysis measurements for the two sensing materials. First black line is the experimental value, the second grey line is the calculated one.

	ICP measurements (scale up)				**Elementary analysis measurements**		
	%w Co exp %w Co clcd	%w P exp %w P clcd	%w Ni exp %w Ni clcd	%w Zr exp %w Zr clcd	%w N exp %w N clcd	%w C exp %w C clcd	%w H exp %w H clcd
CoCorr(2a)@ PCN-222	1.34 0.87	0.36 0.46	3.64 4.42	16.43 20.17	4.04 4.95	45.85 49.00	2.73 2.21
CoCorr(2b)@ PCN-222	1.35 1.54	0.57 0.81	2.59 4.02	12.65 18.33	3.31 5.22	44.99 50.19	3.67 2.14

Molecular formula corresponding to the grafting ratios and metalation ratios, calculated for one porphyrin.

CoCorr(2a)@PCN-222 (Grafting ratio = 0.2): $C_{55.4}H_{30}Zr_3Ni_1Co_{0.2}Cl_{0.8}P_{0.2}N_{4.8}O_{13.8}$

CoCorr(2b)@PCN-222 (Grafting ratio = 0.39): $C_{62.43}H_{31.9}Zr_3Ni_1Co_{0.39}F_{3.12}P_{0.39}N_{5.56}O_{13.61}$

Table S6. Refined parameters calculated for the materials PXRD patterns using Le Bail refinement method on the P6/mmm space group.

Refined Parameters						
Material	a = b (Å)	c (Å)	Alpha = Beta (°)	Gamma (°)	Rp	Rwp
PCN-222	42.1331	16.9293	90	120	4.49	6.94
Activated PCN-222	42.4045	16.7546	90	120	6.5	10.99
Corr(2a)@PCN-222	42.6754	16.7974	90	120	5.25	7.31
Corr(2b)@PCN-222	42.6434	16.6410	90	120	6.75	9.80

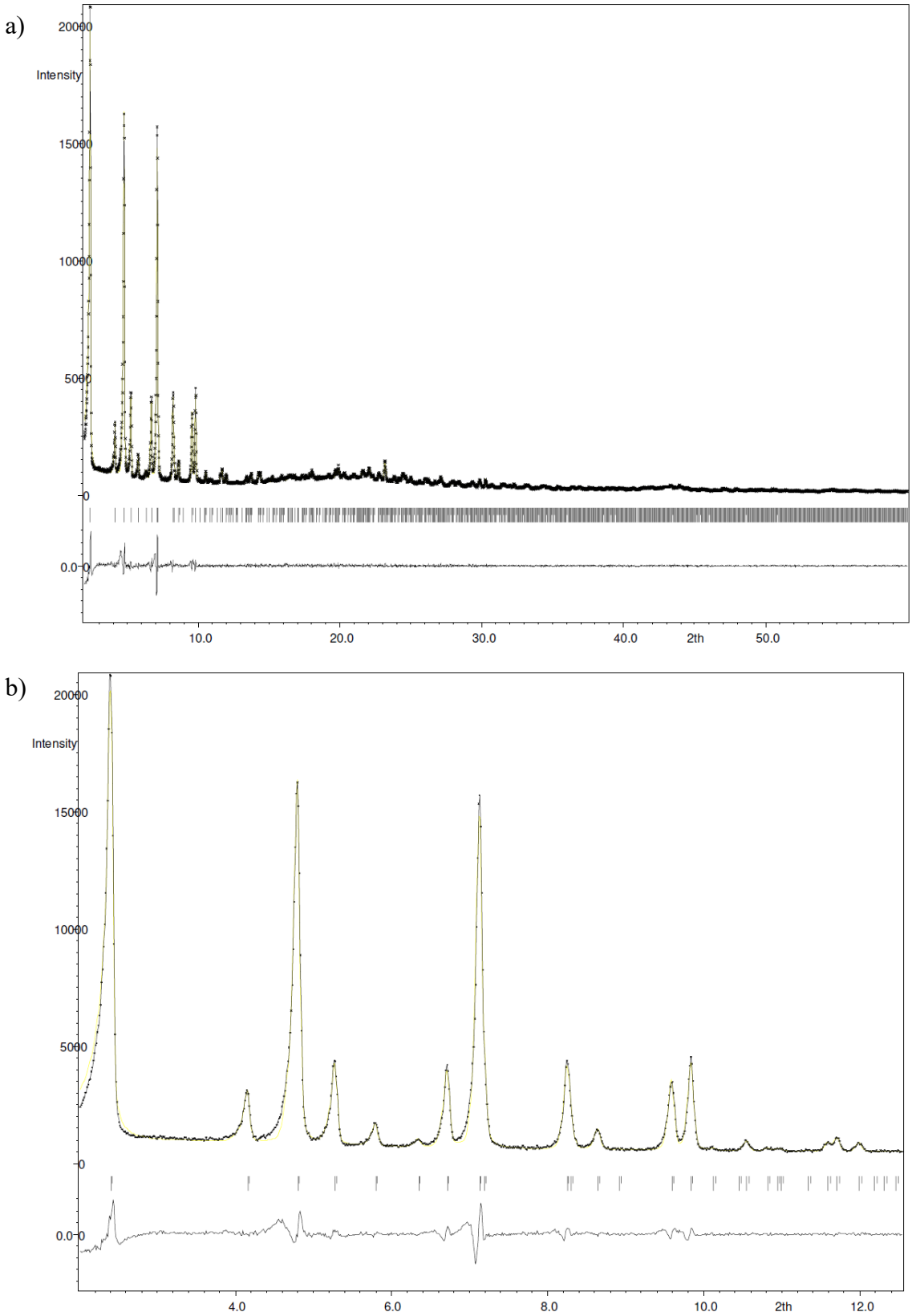

Figure S19. Le Bail fit for **CoCorr(2a)@PCN-222**. Experimental (black) and Le Bail refined (Yellow) a) PXRD Pattern and b) magnification at low angles (2θ degree)

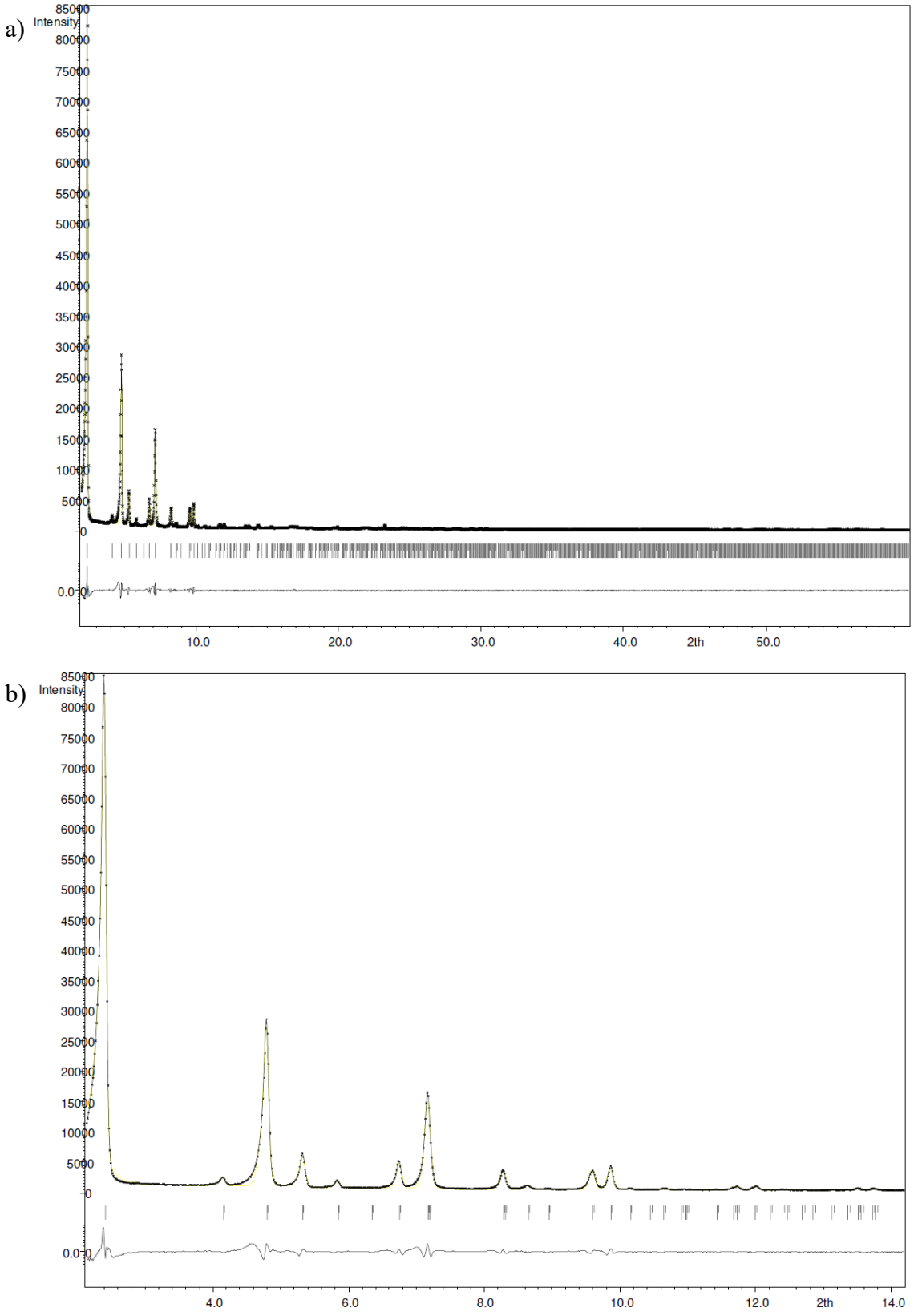

Figure S20. Le Bail fit for **CoCorr(2b)@PCN-222**. Experimental (black) and Le Bail refined (Yellow) a) PXRD Pattern and b) magnification at low angles (2θ degree)

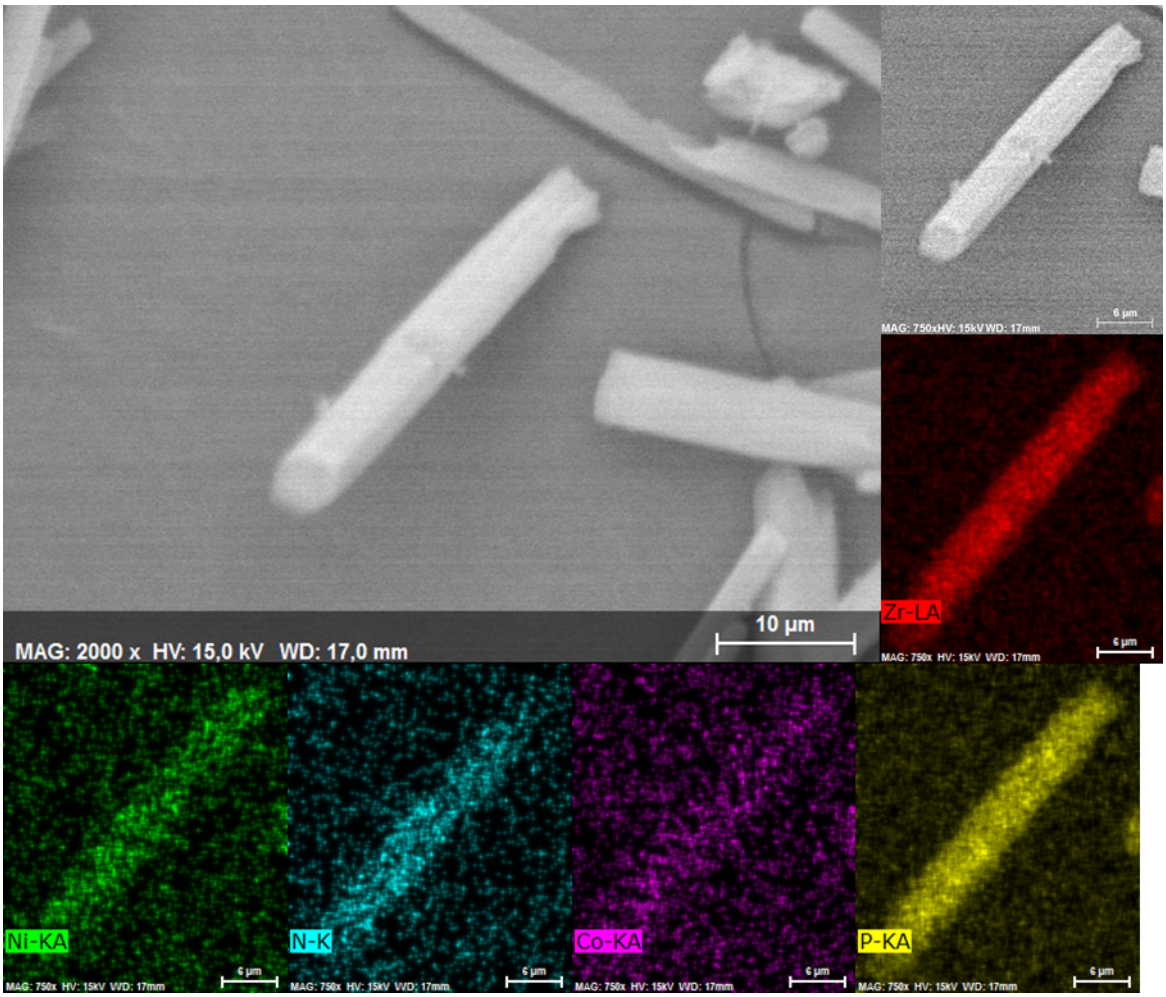

Figure S21. SEM photography and cartography of **CoCorr(2a)@PCN-222**

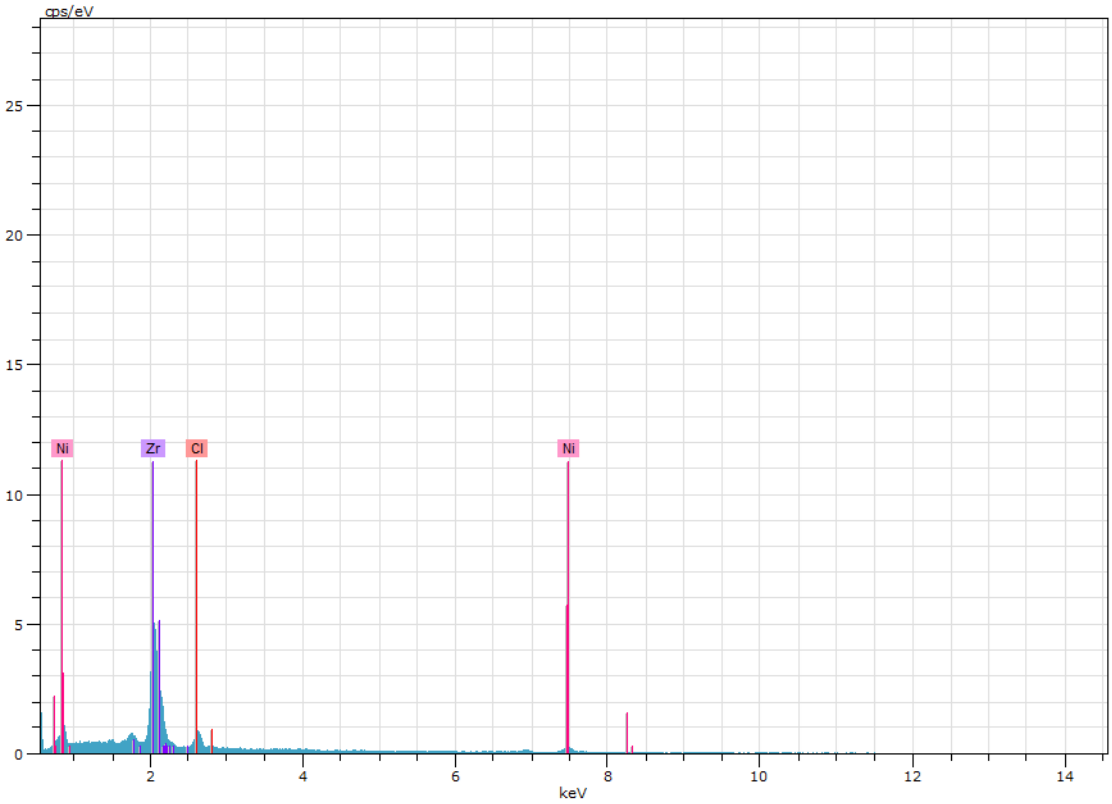

Figure S22. EDX measurements of **CoCorr(2a)@PCN-222**

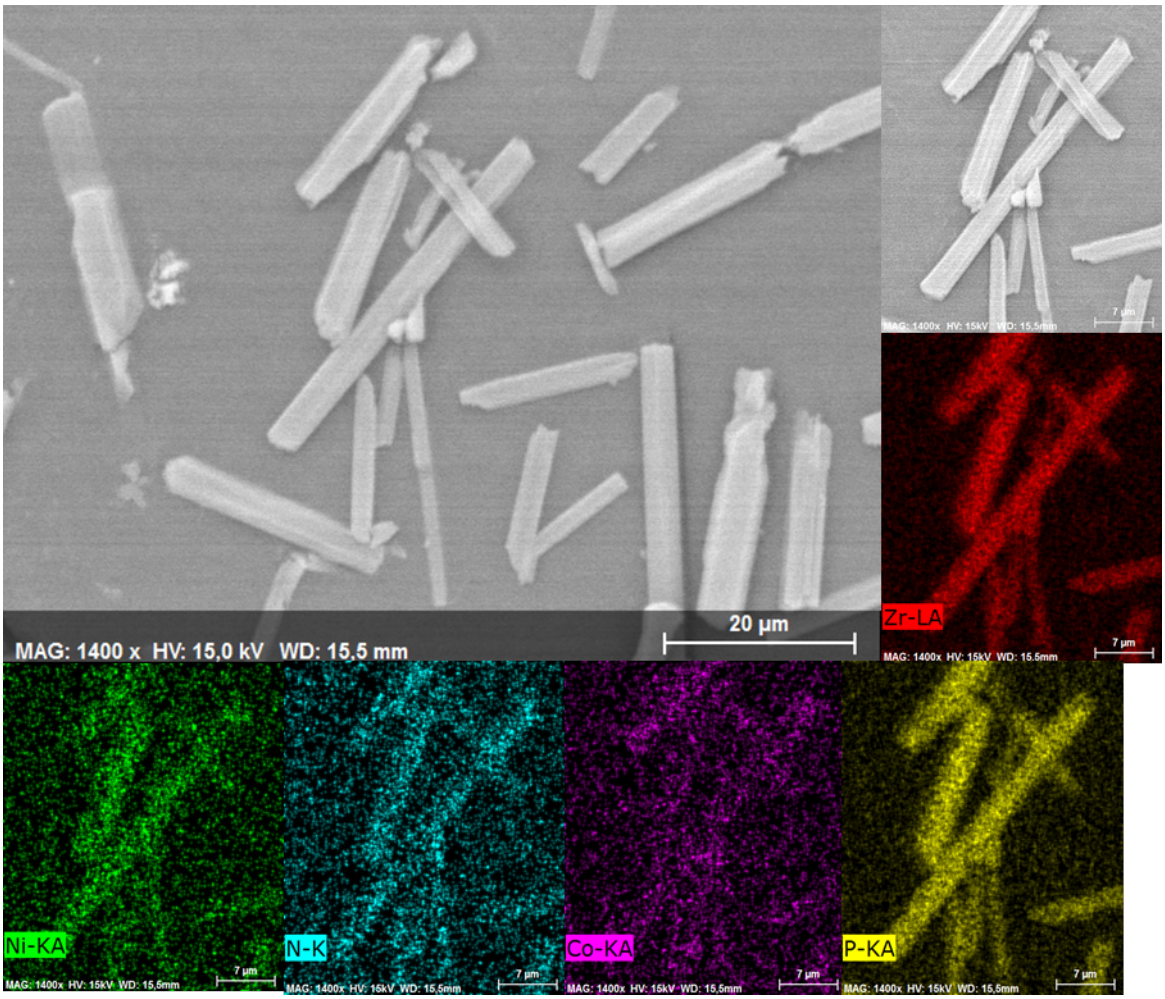

Figure S23. SEM photography and cartography of **CoCorr(2b)@PCN-222**

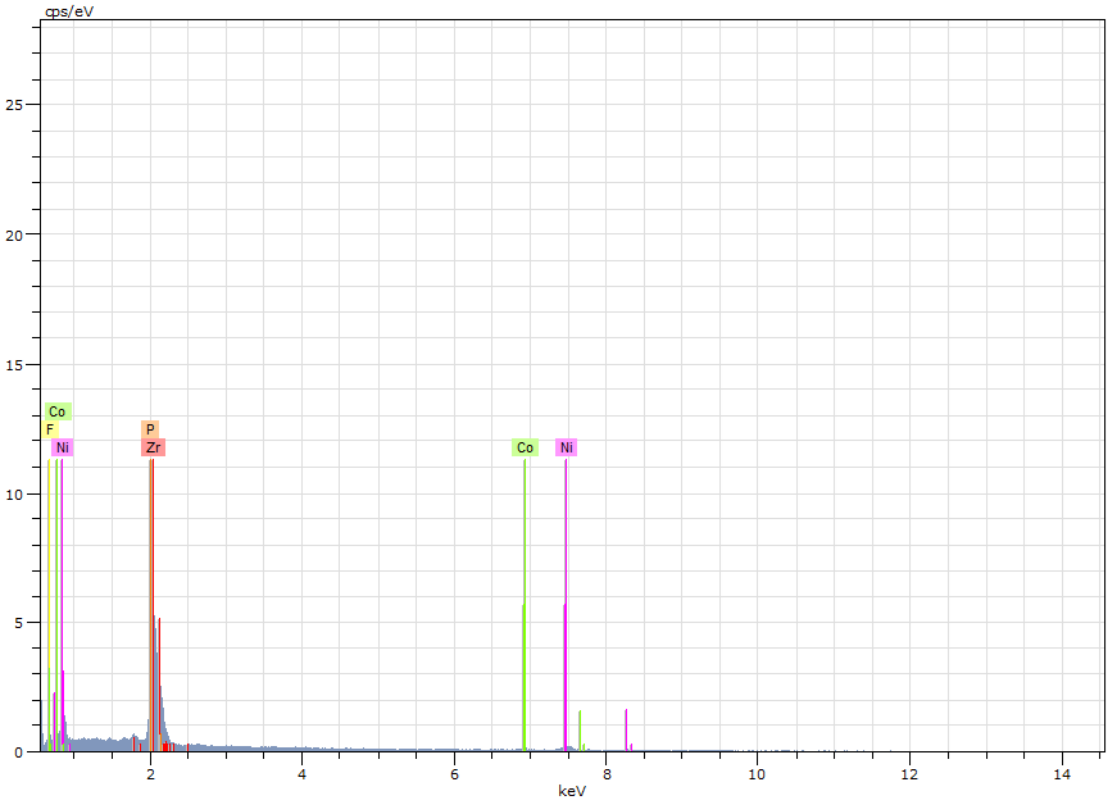

Figure S24. EDX measurements of **CoCorr(2b)@PCN-222**

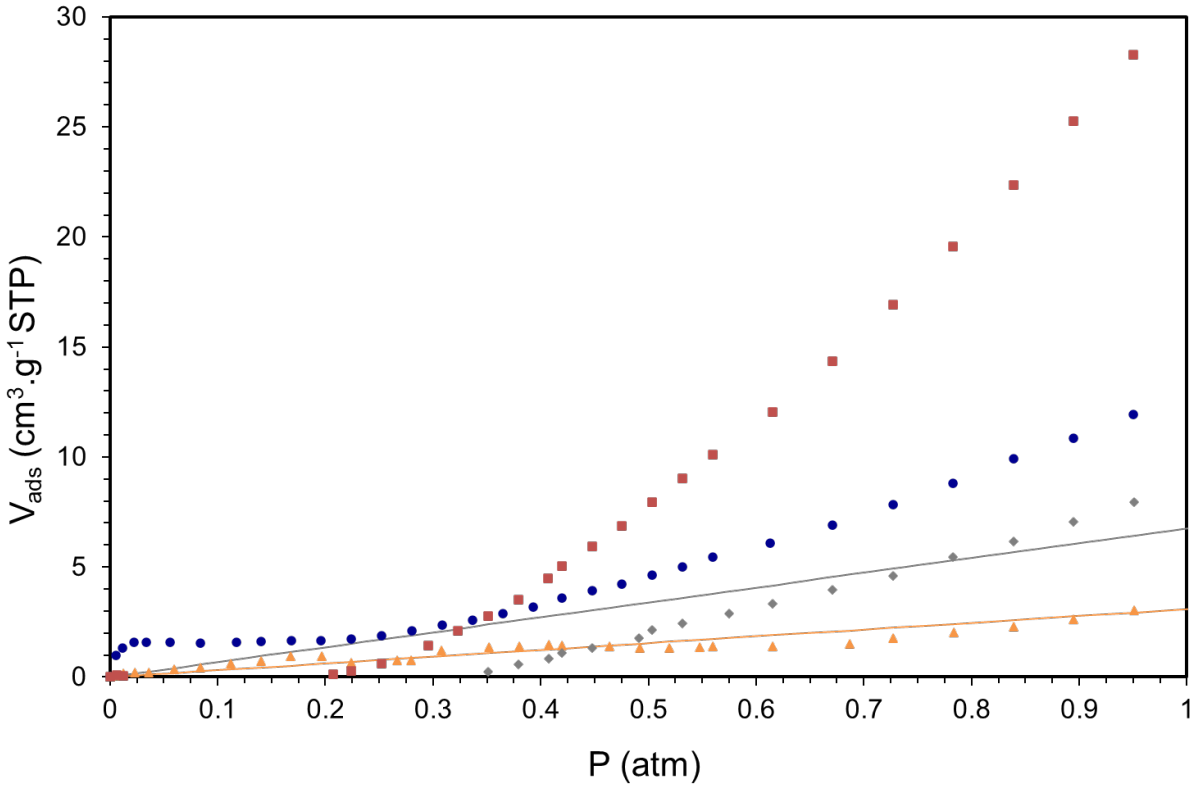

Figure S25. Adsorption isotherm of CO (blue points), CO_2 (red squares), N_2 (yellow triangles) and O_2 (grey rhombuses) recorded at 298 K for **CoCorr(2a)@PCN-222**. Solid lines are the fitting curves of each adsorption using a single-site Langmuir model for N_2 and O_2

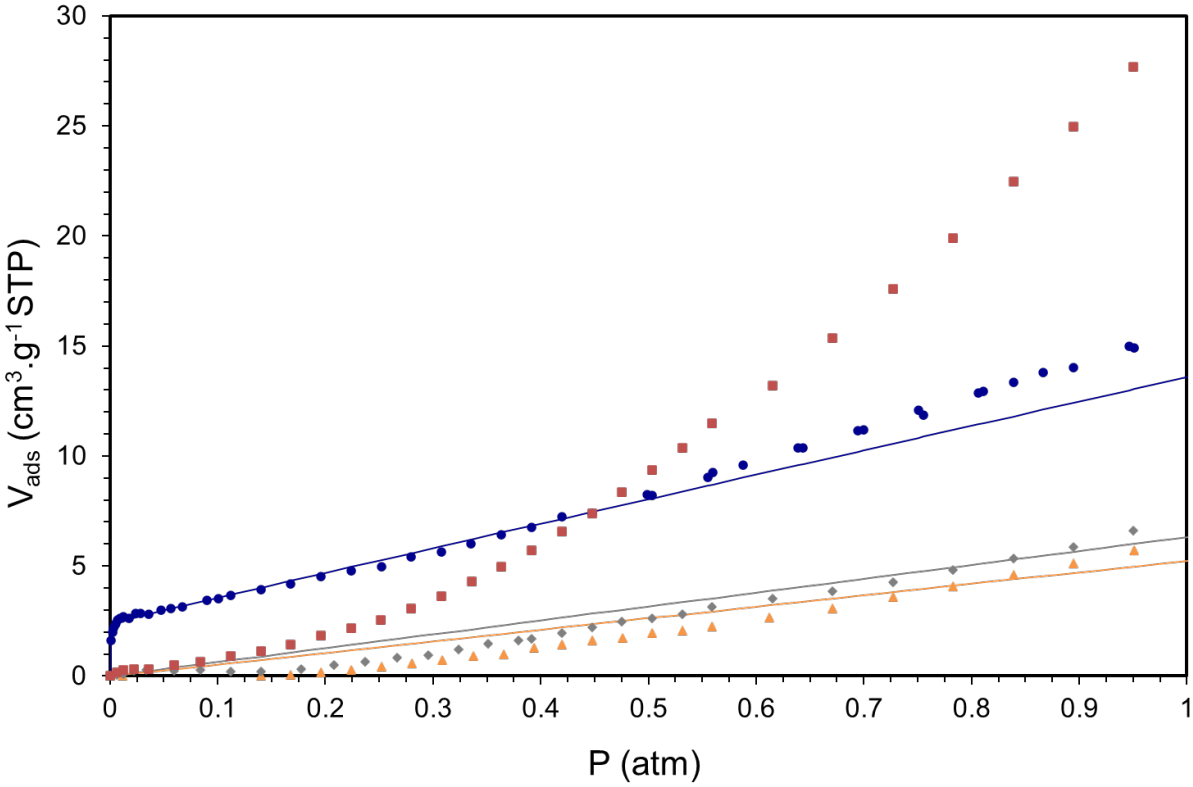

Figure S26. Adsorption isotherm of CO (blue points), CO_2 (red squares), N_2 (yellow triangles) and O_2 (grey rhombuses) recorded at 298 K for **CoCorr(2b)@PCN-222**. Solid lines are the fitting curves of each adsorption using a single-site Langmuir model for N_2, and O_2 and a double-site Langmuir model for CO

Table S7. Fit parameters calculated for the CO isotherms recorded at 298 K

	1st Langmuir component		2nd Langmuir component		
	V_1 a)	K_1 b)	V_2 a)	K_2 b)	$P_{1/2}^{CO}$ c)
CoCorr(2a)@PCN-222	1.54	430	1611.93	$1.02\ 10^{-6}$	$4.70\ 10^{-1}$
CoCorr(2b)@PCN-222	2.45	2149	1125.74	$8.97\ 10^{-3}$	$1.12\ 10^{-3}$

a) Saturation uptake in $cm^3\ g^{-1}$ and b) affinity constants in atm^{-1} estimated from a dual or a triple-site Langmuir model. c) Half-pressure saturation in atm calculated from the two first Langmuir components describing the selective CO sorption on cobalt

Table S8. Henry constants[a)] calculated from the N_2, O_2 and CO_2 at 298 K

	N_2	O_2	CO_2
	V_{N2} [b)] x K_{N2} [c)]	V_{O2} [b)] x K_{O2} [c)]	V_{CO2} [b)] x K_{CO2} [c)]
CoCorr(2a)@PCN-222	3.09	6.79	25.14
CoCorr(2b)@PCN-222	5.27	6.34	25.76

[a)] Expressed in $cm^3\ g^{-1}\ atm^{-1}$. [b)] Saturation uptakes and [c)] affinity constant estimated from a single-site Langmuir model.

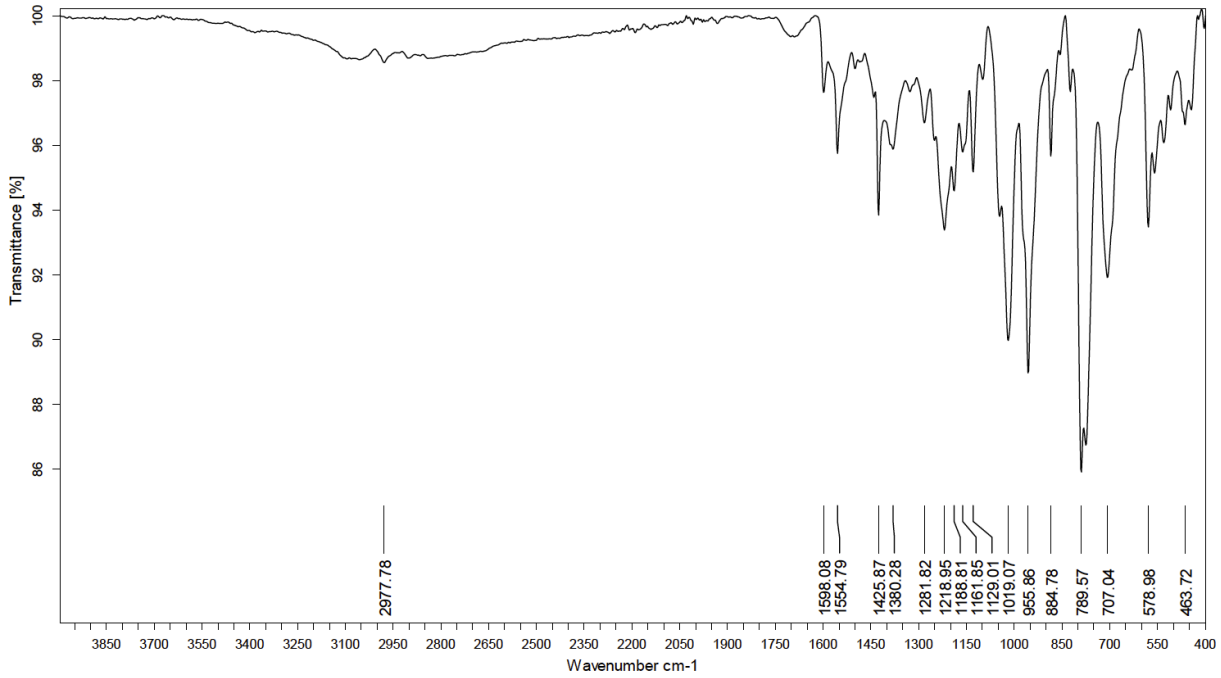

Figure S27. IR spectrum (KBr) of corrole **1a**

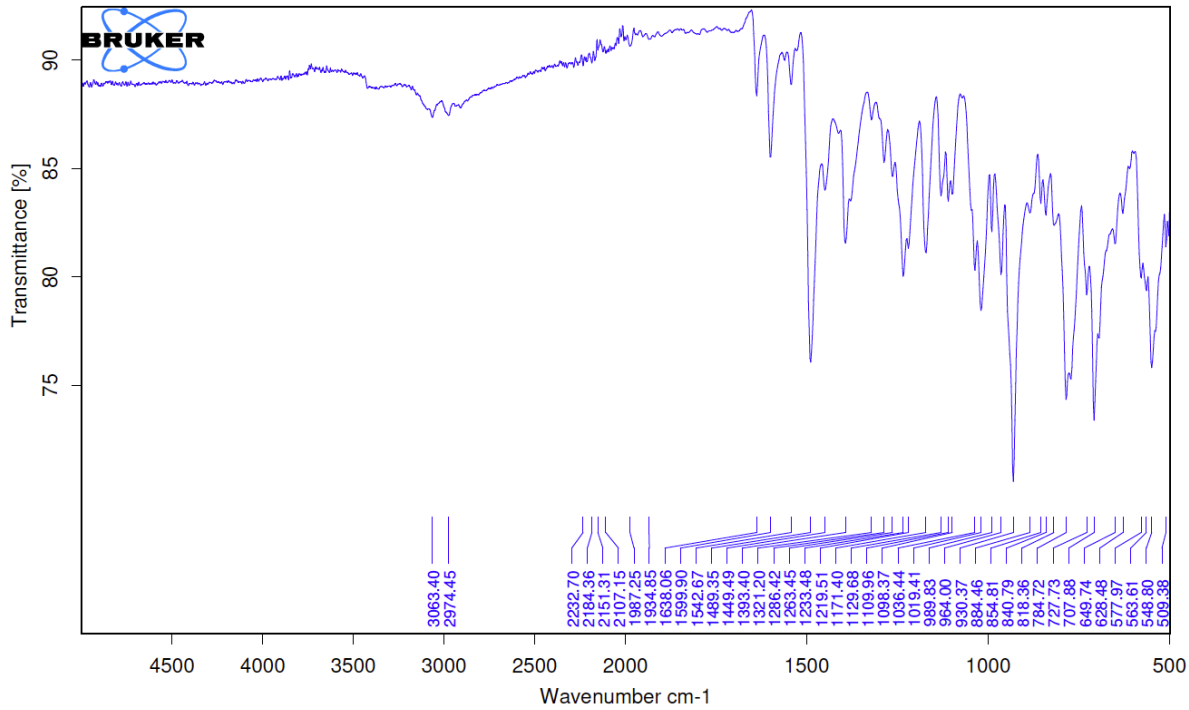

Figure S28. IR spectrum (KBr) of corrole **1b**

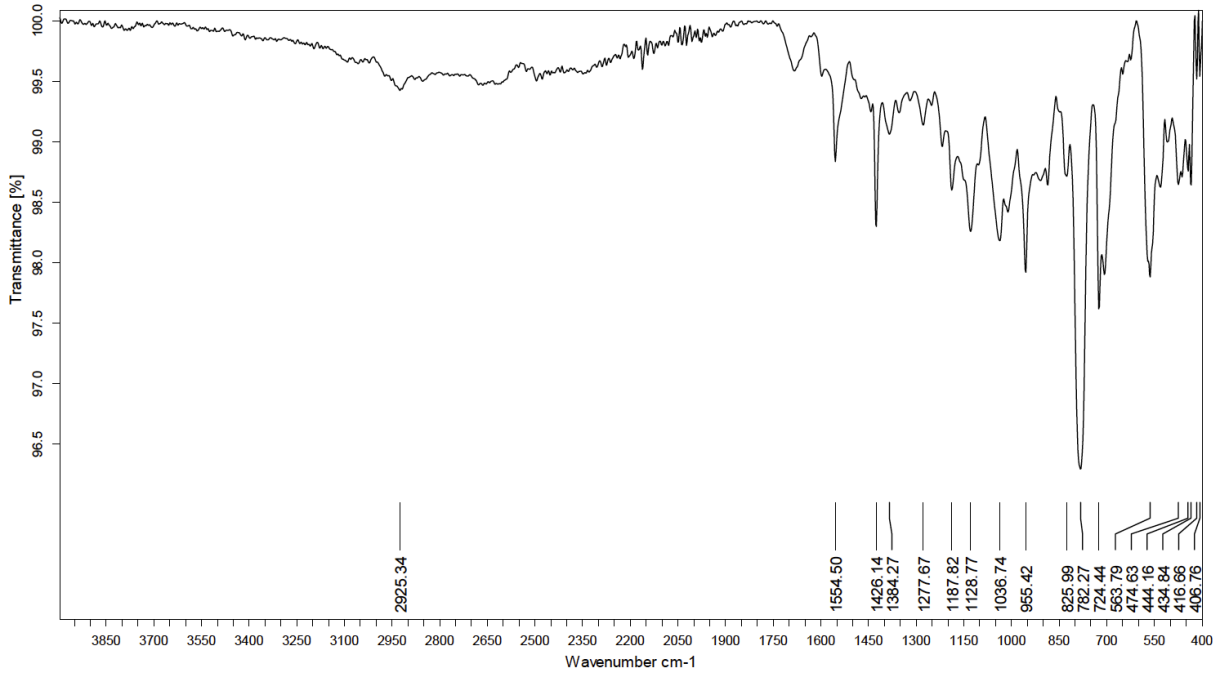

Figure S29. IR spectrum (KBr) of corrole **2a**

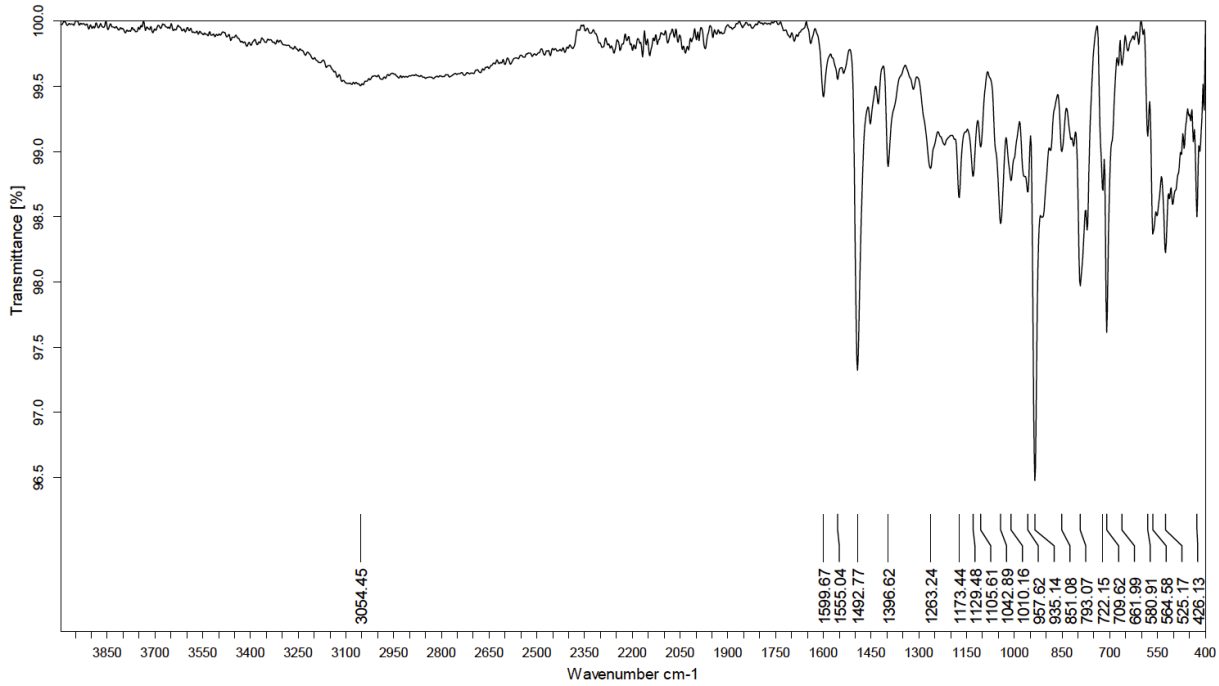

Figure S30. IR spectrum (KBr) of corrole **2b**

References

[1] K. S. Walton, R. Q. Snurr, *J. Am. Chem. Soc.* **2007**, *129*, 8552-8556.

[2] J. Rouquerol, P. Llewellyn, F. Rouquerol, *Stud. Surf. Sci. Catal.* **2007**, 49-56.

[3] M. Maares, M. M. Ayhan, K. B. Yu, A. O. Yazaydin, K.Harmandar, H. Haase, J. Beckmann, Y. Zorlu and G. Yücesan, *Chem. Eur. J*. **2019**, *25*, 11214-11217

[4] B. Koszarna and D. T. Gryko, *J. Org. Chem*. **2006**, *71*, 3707-3717

[5] S. Kepler-Gratias, L. Bucher, S. Sokunthea, C. Quentin-Froignant, N. Desbois, S. Bertagnoli, M. Louison, E. Monge, A. Bousquet-Melou, M. Lacroix, C. P. Gros, F. Gallardo, *ACS Inf. Dis.*, **2021**, *7 (8),* 2370 -2382

[6] Bruker, *SAINT*, *V8.40B*, Bruker AXS Inc., Madison, Wisconsin, USA.

[7] L. Krause, R. Herbst-Irmer, G. M. Sheldrick, D. Stalke, *J. Appl. Cryst.* **2015**, *48*, 3–10.

[8] G. M. Sheldrick, *Acta Cryst.* **2015**, *A71*, 3–8, doi:10.1107/S2053273314026370.

[9] G. M. Sheldrick, *Acta Cryst.* **2015**, *C71*, 3–8, doi:10.1107/S2053229614024218.

[10] C. R. Groom, I. J. Bruno, M. P. Lightfoot, S. C. Ward, *Acta Cryst.* **2016**, *B72*, 171–179.

[11] D. Kratzert, *FinalCif*, *V139*, https://dkratzert.de/finalcif.html

[12] L. Zeng, P. Liao, H. Liu, L. Liu, Z. Liang, J. Zhang, L. Chen, C.-Y. Su, *J. Mater. Chem. A* **2016,** *4* (21), 8328-8336.